Status of non-standard neutrino interactions

Tommy Ohlsson*

Department of Theoretical Physics, School of Engineering Sciences,

KTH Royal Institute of Technology – AlbaNova University Center,

Roslagstullsbacken 21, 106 91 Stockholm, Sweden

(Dated: September 14, 2012)

Abstract

The phenomenon of neutrino oscillations has been established as the leading mechanism behind neutrino flavor transitions, providing solid experimental evidence that neutrinos are massive and lepton flavors are mixed. Here we review sub-leading effects in neutrino flavor transitions known as non-standard neutrino interactions, which is currently the most explored description for effects beyond the standard paradigm of neutrino oscillations. Especially, we report on the phenomenology of non-standard neutrino interactions and their experimental and phenomenological bounds as well as future sensitivity and discovery reach.

PACS numbers: 13.15.+g, 14.60.Pq, 14.60.St

* tohlsson@kth.se

I. INTRODUCTION

Since the results of the Super-Kamiokande experiment in Japan in 1998 [1], the phenomenon of neutrino oscillations has been established as the leading mechanism behind neutrino flavor transitions. This result was followed by a first boom of results from several international collaborations (e.g. SNO, KamLAND, K2K, MINOS, and MiniBooNE) on the various neutrino parameters. Certainly, these solid results have pinned down the values on the different parameters to an incredible precision given that neutrinos are very elusive particles and the corresponding experiments are extraordinarily complex (see Ref. [2]). Nevertheless, it is a fact that the present Standard Model (SM) of particle physics is not the whole story and needs to be revised in order to accommodate massive and mixed neutrinos, which leads to physics beyond the SM. With the upcoming results from the running or future neutrino experiments (e.g. Daya Bay, Double Chooz, RENO, KATRIN, T2K, NOνA, OPERA, ICARUS), there will be a second boom of results, and we will hopefully be able to determine the missing neutrino parameters such as the leptonic CP-violating phase (important for the matter-antimatter asymmetry in the Universe), the sign of the large mass-squared difference for neutrinos (important for the neutrino mass hierarchy), and the absolute neutrino mass scale, but also the next-to-leading order effects in neutrino flavor transitions.

In future neutrino experiments (and in particular for a neutrino factory, β-beams, or superbeams), new physics beyond the SM may appear in the form of unknown couplings involving neutrinos, which are usually referred to as non-standard neutrino interactions (NSIs). Compared to standard neutrino oscillations, NSIs could contribute to the oscillation probabilities and neutrino event rates as sub-leading effects, and may bring in very distinctive phenomena. Running and future neutrino experiments will provide us with more precision measurements on neutrino flavor transitions, and therefore, the window of searching for NSIs is open. In principle, NSIs could exist in the neutrino production, propagation, and detection processes, and the search for NSIs is complementary to the direct search for new physics conducted at the LHC.

The concept of NSIs has been introduced in order to accommodate for sub-leading effects in neutrino flavor transitions. Previously, alternative scenarios for neutrino flavor transitions such as neutrino decoherence, neutrino decay, and NSIs have been studied (see below for references), but now, such alternatives are only allowed to provide sub-leading effects to

neutrino oscillations. In the literature, there exist several theoretical and phenomenological studies of NSIs for atmospheric, accelerator, reactor, solar, and supernova neutrinos. In addition, some experimental collaborations have obtained bounds on NSIs.

This review is organized as follows. In Section II, we introduce the concept of neutrino flavor transitions with NSIs. First, we present standard neutrino oscillations, and then, we consider other scenarios for neutrino flavor transitions including NSIs. At the end of this section, we discuss so-called NSI Hamiltonian effects of neutrino oscillations. Then, in Section III, we describe NSIs with three neutrino flavors, since there are at least three flavors in Nature. Especially, we consider production, propagation, and detection NSIs including the so-called zero-distance effect. In addition, we present mappings for NSIs and approximate formulas for two neutrino flavors that can be useful in some settings. Next, in Section IV, we study different theoretical models for NSIs including e.g. see-saw models. In Section V, we investigate the phenomenology of NSIs for different types of neutrinos such as atmospheric, accelerator, reactor, solar, and supernova neutrinos, whereas in Section VI, we review phenomenological bounds on NSIs. In addition, in Section VII, we examine experimental sensitivities and the future discovery reach of NSIs. Finally, in Section VIII, we present a summary and state our conclusions.

II. NEUTRINO FLAVOR TRANSITIONS WITH NSIS

In this section, we present the basic ingredients for neutrino oscillations (based on the two facts that neutrinos are massive and lepton flavors are mixed), which is the leptonic mixing matrix, a Schrödinger-like equation for the evolution of the neutrinos, and the values of the fundamental neutrino oscillations parameters, i.e., the neutrino mass-squared differences and the leptonic mixing parameters. Then, we discuss some historic alternative scenarios for neutrino flavor transitions. Finally, we study NSI Hamiltonian effects of neutrino oscillations.

A. Neutrino oscillations

Indeed, there are now strong evidences that neutrinos are massive and lepton flavors are mixed. In the SM, neutrinos are massless particle, and therefore, the SM must be extended by adding neutrino masses. The lepton flavor mixing is usually defined through the leptonic

mixing matrix U that can be written as

$$\begin{pmatrix} \nu_e \\ \nu_\mu \\ \nu_\tau \end{pmatrix} = U \begin{pmatrix} \nu_1 \\ \nu_2 \\ \nu_3 \end{pmatrix} = \begin{pmatrix} U_{e1} & U_{e2} & U_{e3} \\ U_{\mu 1} & U_{\mu 2} & U_{\mu 3} \\ U_{\tau 1} & U_{\tau 2} & U_{\tau 3} \end{pmatrix} \begin{pmatrix} \nu_1 \\ \nu_2 \\ \nu_3 \end{pmatrix} , \tag{1}$$

which relates the weak interaction eigenstates and the mass eigenstates through the leptonic mixing parameters θ_{12}, θ_{13}, θ_{23}, δ (the Dirac CP-violating phase), as well as ρ and σ (the Majorana CP-violating phases). In the so-called standard parameterization, U is given by

$$U = \begin{pmatrix} 1 & 0 & 0 \\ 0 & c_{23} & s_{23} \\ 0 & -s_{23} & c_{23} \end{pmatrix} \begin{pmatrix} c_{13} & 0 & s_{13}\mathrm{e}^{-\mathrm{i}\delta} \\ 0 & 1 & 0 \\ -s_{13}\mathrm{e}^{\mathrm{i}\delta} & 0 & c_{13} \end{pmatrix} \begin{pmatrix} c_{12} & s_{12} & 0 \\ -s_{12} & c_{12} & 0 \\ 0 & 0 & 1 \end{pmatrix} \begin{pmatrix} \mathrm{e}^{\mathrm{i}\rho} & 0 & 0 \\ 0 & \mathrm{e}^{\mathrm{i}\sigma} & 0 \\ 0 & 0 & 1 \end{pmatrix} , \tag{2}$$

where $c_{ij} \equiv \cos(\theta_{ij})$ and $s_{ij} \equiv \sin(\theta_{ij})$.

The time evolution of the neutrino vector of state $\nu = \begin{pmatrix} \nu_e & \nu_\mu & \nu_\tau \end{pmatrix}^T$ describing neutrino oscillations is given by a Schrödinger-like equation with a Hamiltonian H, namely,

$$\mathrm{i}\frac{\mathrm{d}\nu}{\mathrm{d}t} = \frac{1}{2E}\left[MM^\dagger + \mathrm{diag}(A,0,0)\right]\nu \equiv H\nu\,, \tag{3}$$

where E is the neutrino energy, $M = U\,\mathrm{diag}(m_1, m_2, m_3)\,U^T$ is the neutrino mass matrix, and $A = 2\sqrt{2}EG_FN_e$ is the effective matter potential induced by ordinary charged-current interactions with electrons [3, 4]. Here, m_1, m_2, and m_3 are the definite masses of the neutrino mass eigenstates and N_e is the electron density of matter along the neutrino trajectory. Quantum mechanically, the transition probability amplitudes are given as overlaps of different neutrino states, and finally, neutrino oscillation probabilities are defined as squared absolute values of the transition probability amplitudes. Thus, flavor transitions occur during the evolution of neutrinos. For example, in a two-flavor illustration (in vacuum) with electron and muon neutrinos, a neutrino state can be in a pure electron neutrino state at one time, whereas it can be in a pure muon neutrino state at another time.

Using global fits of data from neutrino oscillation experiments (and especially, results from long-baseline neutrino experiments including matter effects), the values given in Table I have been obtained for the fundamental neutrino oscillation parameters [5]. Note that these values have been found without taking sub-leading effects such as NSIs into account. Open questions that still exist are: Are neutrinos Dirac or Majorana particles? What is the absolute neutrino mass scale? What is the sign of the large mass-squared difference Δm^2_{31}?

parameter	best-fit value	3σ range
Δm^2_{21} $[10^{-5}\,\mathrm{eV}^2]$	7.50 ± 0.185	$7.00 \div 8.09$
$\lvert\Delta m^2_{31}\rvert$ $[10^{-3}\,\mathrm{eV}^2]$	$2.45^{+0.067}_{-0.071}$	$2.25 \div 2.67$
$\sin^2(\theta_{12})$	$0.30^{+0.013}_{-0.012}$	$0.27 \div 0.34$
$\sin^2(\theta_{13})$	0.023 ± 0.0023	$0.016 \div 0.030$
$\sin^2(\theta_{23})$	$0.42^{+0.037}_{-0.031}$	$0.39 \div 0.66$

TABLE I. Present values of the fundamental neutrino oscillation parameters. See also Refs. [6, 7] for two other global analyses.

Is there leptonic CP violation? Do sterile neutrinos exist? However, recently, one has also been concerned with the following two questions in the literature: Are there NSIs? Is there non-unitarity in leptonic mixing? The intention of this review is to bring some insight into these last two questions (with emphasis on the first question).

B. Other scenarios for neutrino flavor transitions

The Super-Kamiokande, SNO, and KamLAND experiments have provided strong evidence for neutrino flavor transitions and that the theory of neutrino oscillations is the leading description [1, 8, 9]. In various neutrino oscillation experiments, precision measurements for some of the neutrino parameters, i.e., Δm^2_{21}, $|\Delta m^2_{31}|$, θ_{12}, θ_{13}, and θ_{23}, have been obtained, whereas other parameters are still completely unknown such as $\mathrm{sign}(\Delta m^2_{31})$ and δ, as well as the Majorana CP-violating phases and the absolute neutrino mass scale.

Other mechanisms could be responsible for flavor transitions on a sub-leading level (see e.g. Ref. [10]). Therefore, we will phenomenologically study "new physics" effects due to NSIs. In the past, descriptions for transitions of neutrinos based on neutrino decoherence and neutrino decay have been extensively investigated in the literature [11–53]. However, now, such descriptions are ruled out by available neutrino data as the leading-order mechanism behind neutrino flavor transitions [23, 54–57], but these descriptions could still provide sub-leading effects. In what follows, I will not consider neutrino decoherence and neutrino decay, but instead focus on NSIs, which are interactions between neutrinos and matter fermions (i.e., u, d, and e) that additionally affect neutrino oscillations, as a sub-leading mechanism for neutrino flavor transitions.

C. NSI Hamitonian effects of neutrino oscillations

In general, NSIs can be considered to be effective additional contributions to the standard vacuum Hamiltonian H_0 that describes the neutrino evolution (see e.g. Ref. [58]). Thus, any Hermitian non-standard Hamiltonian effect H' will alter the original Hamiltonian into an effective Hamiltonian:

$$H_{\rm eff} = H_0 + H' \,. \tag{4}$$

For example, neutrino oscillations in matter are described by

$$H' = H_{\rm matter} = \frac{1}{2E}{\rm diag}(A, 0, \ldots, 0) - \frac{1}{\sqrt{2}} G_F N_n \mathbb{1}_n \,, \tag{5}$$

where G_F is the Fermi weak coupling constant, N_n is the nucleon number density, and $\mathbb{1}_n$ is the $n \times n$ unit matrix. Just as the presence of matter affects the effective neutrino parameters, the effective neutrino parameters will be affected by any non-standard Hamiltonian effect. The non-standard Hamiltonian effects can alter both the oscillation frequency and the oscillation amplitude and they can be classified as "flavor effects" or "mass effects" [58]. Furthermore, non-standard Hamiltonian effects (such as NSIs) will lead to resonance conditions [58], which are modified (and more general) versions of the famous Mikheyev–Smirnow–Wolfenstein effect [3, 4, 59].

III. NSIS WITH THREE NEUTRINO FLAVORS

The phenomenological consequences of NSIs have been investigated in great detail in the literature. The widely studied operators responsible for NSIs can be written as [3, 60–62]

$$\mathcal{L}_{\rm NSI} = -2\sqrt{2} G_F \varepsilon_{\alpha\beta}^{ff'C} \left(\overline{\nu_\alpha} \gamma^\mu P_L \nu_\beta\right) \left(\overline{f} \gamma_\mu P_C f'\right) \,, \tag{6}$$

where $\varepsilon_{\alpha\beta}^{ff'C}$ are NSI parameters, $\alpha, \beta = e, \mu, \tau$, $f, f' = e, u, d$, and $C = L, R$. Note that these operators are non-renormalizable and they are also not gauge invariant. Thus, using the NSI operators in Eq. (6), we find that the effective NSI parameters are

$$\varepsilon_{\alpha\beta} \propto \frac{m_W^2}{m_X^2} \,, \tag{7}$$

where m_W is the W boson mass and m_X is the mass scale of the NSIs. If the new physics scale, i.e., the NSI scale, is of the order of 1(10) TeV, then one obtains $\varepsilon_{\alpha\beta} \sim 10^{-2}(10^{-4})$.

In principle, NSIs can affect both (i) production and detection processes and (ii) propagation in matter, and one can have combination of both effects. In the following, we will first study production and detection NSIs, including the so-called zero-distance effect, and then matter NSIs. In addition, we will present mappings with NSIs and discuss approximate formulas for two neutrino flavors.

A. Production and detection NSIs and the zero-distance effect

In general, production and detection processes can be affected by NSIs, and for a realistic neutrino oscillation experiment, the neutrino states produced in a source and observed at a detector can be written as superpositions of pure orthonormal flavor eigenstates [60, 63–65]:

$$|\nu_\alpha^s\rangle = |\nu_\alpha\rangle + \sum_{\beta=e,\mu,\tau} \varepsilon_{\alpha\beta}^s |\nu_\beta\rangle = (1+\varepsilon^s) U |\nu_m\rangle \,, \tag{8}$$

$$\langle\nu_\beta^d| = \langle\nu_\beta| + \sum_{\alpha=e,\mu,\tau} \varepsilon_{\alpha\beta}^d \langle\nu_\alpha| = \langle\nu_m| U^\dagger [1+(\varepsilon^d)^\dagger] \,, \tag{9}$$

where the superscripts 's' and 'd' denote the source and the detector, respectively, and $|\nu_m\rangle$ is a neutrino mass eigenstate. Note that the states $|\nu_\alpha^s\rangle$ and $\langle\nu_\beta^d|$ are not orthonormal states due to the NSIs and that the matrices ε^s and ε^d are not necessarily the same matrix, since different physical processes take place at the source and the detector, which means that these matrices are arbitrary and non-unitary in general. If the production and detection processes are exactly the same process with the same participating fermions (e.g. β-decay and inverse β-decay), then the same matrix enters as $\varepsilon^s = \left(\varepsilon^d\right)^\dagger$, or on the form of matrix elements, $\varepsilon_{\alpha\beta}^s = \varepsilon_{\alpha\beta}^d = (\varepsilon_{\beta\alpha}^s)^* = (\varepsilon_{\beta\alpha}^d)^*$ [66]. For example, in the case of so-called non-unitarity effects (which can be considered as a type of NSIs, see e.g. Ref. [67]) in the minimal unitarity violation model [68–73], it holds that $\varepsilon^s = \left(\varepsilon^d\right)^\dagger$. Thus, it is important to keep in mind that these matrices are experiment- and process-dependent quantities.

In the case of production and detection NSIs, the neutrino transition probabilities are

given by [65, 74]

$$
\begin{aligned}
P(\nu_\alpha^s \to \nu_\beta^d; L) &= \left| \sum_{\gamma,\delta,i} \left(1+\varepsilon^d\right)_{\gamma\beta} \left(1+\varepsilon^s\right)_{\alpha\delta} U_{\delta i} U_{\gamma i}^* \, \mathrm{e}^{-\mathrm{i}\frac{m_i^2 L}{2E}} \right|^2 \\
&= \sum_{i,j} \mathcal{J}_{\alpha\beta}^i \mathcal{J}_{\alpha\beta}^{j*} - 4 \sum_{i>j} \mathrm{Re}(\mathcal{J}_{\alpha\beta}^i \mathcal{J}_{\alpha\beta}^{j*}) \sin^2\left(\frac{\Delta m_{ij}^2 L}{4E}\right) \\
&\quad + 2 \sum_{i>j} \mathrm{Im}(\mathcal{J}_{\alpha\beta}^i \mathcal{J}_{\alpha\beta}^{j*}) \sin\left(\frac{\Delta m_{ij}^2 L}{2E}\right) \,, \qquad (10)
\end{aligned}
$$

where

$$
\mathcal{J}_{\alpha\beta}^i = U_{\alpha i}^* U_{\beta i} + \sum_\gamma \varepsilon_{\alpha\gamma}^s U_{\gamma i}^* U_{\beta i} + \sum_\gamma \varepsilon_{\gamma\beta}^d U_{\alpha i}^* U_{\gamma i} + \sum_{\gamma,\delta} \varepsilon_{\alpha\gamma}^s \varepsilon_{\delta\beta}^d U_{\gamma i}^* U_{\delta i} \,. \qquad (11)
$$

In fact, an important feature of Eq. (10) is that when $\alpha \neq \beta$, the first term is generally non-vanishing, which means that a neutrino flavor transition would already happen at the source before the oscillation process has taken place. This is known as the *zero-distance effect* [75]. It could be measured with a near detector close to the source. Note that Eq. (10) is also usable to describe neutrino oscillations with a non-unitary mixing matrix, e.g. in the minimal unitarity violation model [68].

B. Matter NSIs

In order to describe neutrino propagation in matter with NSIs, the simple effective matter potential in Eq. (3) needs to be extended. Similar to standard matter effects, NSIs can affect the neutrino propagation by coherent forward scattering in Earth matter. The Earth matter effects are more or less involved depending on the specific terrestrial neutrino oscillation experiment. In other words, the Hamiltonian in Eq. (3) is replaced by an effective Hamiltonian, which governs the propagation of neutrino flavor states in matter with NSIs, viz. [3, 76–78]

$$
\tilde{H} = \frac{1}{2E} \left[U \mathrm{diag}(m_1^2, m_2^2, m_3^2) U^\dagger + \mathrm{diag}(A, 0, 0) + A\varepsilon^m \right] \,, \qquad (12)
$$

where the matrix ε^m contains the (effective) NSI parameters $\varepsilon_{\alpha\beta}$, which are defined as

$$
\varepsilon_{\alpha\beta} = \sum_{f,P} \varepsilon_{\alpha\beta}^{fP} \frac{N_f}{N_e} \qquad (13)
$$

with the parameters $\varepsilon_{\alpha\beta}^{fP}$ being entries of the Hermitian matrix ε^{fP} and giving the strengths of the NSIs and the quantity N_f being the number density of a fermion of type f. Unlike

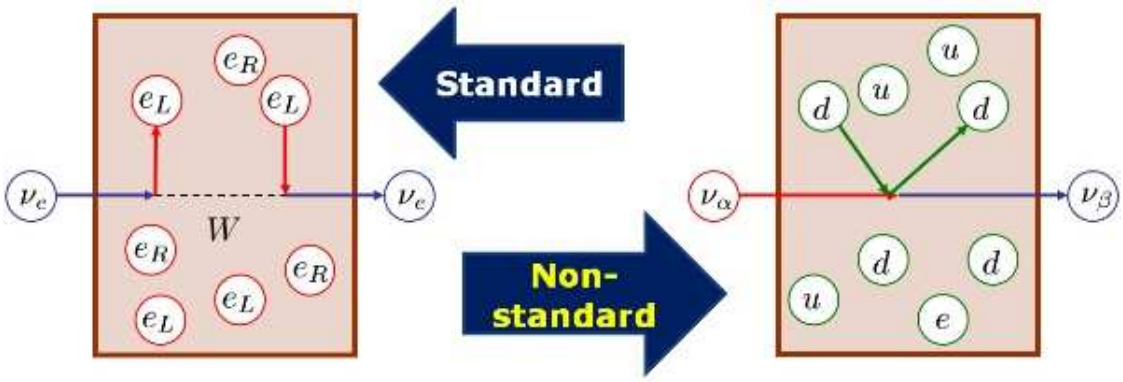

FIG. 1. Schematic pictures of standard matter effects (left picture) and matter non-standard neutrino interactions (right picture).

ε^s and ε^d, ε^m is a Hermitian matrix describing NSIs in matter, where the superscript 'm' is used to distinguish matter NSIs from production and detection NSIs. Thus, for three neutrino flavors, we obtain

$$\mathrm{i}\frac{\mathrm{d}}{\mathrm{d}t}\begin{pmatrix}\nu_e\\ \nu_\mu\\ \nu_\tau\end{pmatrix} = \frac{1}{2E}\left[U\begin{pmatrix}0 & 0 & 0\\ 0 & \Delta m^2_{21} & 0\\ 0 & 0 & \Delta m^2_{31}\end{pmatrix}U^\dagger + A\begin{pmatrix}1+\varepsilon_{ee} & \varepsilon_{e\mu} & \varepsilon_{e\tau}\\ \varepsilon^*_{e\mu} & \varepsilon_{\mu\mu} & \varepsilon_{\mu\tau}\\ \varepsilon^*_{e\tau} & \varepsilon^*_{\mu\tau} & \varepsilon_{\tau\tau}\end{pmatrix}\right]\begin{pmatrix}\nu_e\\ \nu_\mu\\ \nu_\tau\end{pmatrix} . \tag{14}$$

The "1" in the 1-1-element of the effective matter potential in Eq. (14) describes the interaction of electron neutrinos with left-handed electrons through the exchange of W bosons, i.e., the standard matter interactions, whereas the NSI parameters $\varepsilon_{\alpha\beta}$ in the effective matter potential describe the matter NSIs. See Fig. 1 for schematic pictures of standard and non-standard matter effects. Now, the effective Hamiltonian $\tilde{H}$ in Eq. (12) can be diagonalized using a unitary transformation, and one finds

$$\tilde{H} = \frac{1}{2E}\hat{U}\mathrm{diag}(\hat{m}^2_1, \hat{m}^2_2, \hat{m}^2_3)\hat{U}^\dagger\,, \tag{15}$$

where $\hat{m}^2_i$ $(i = 1, 2, 3)$ denote the effective mass-squared eigenvalues of neutrinos and $\hat{U}$ is the effective leptonic mixing matrix in matter. Explicit expressions for these quantities can be found in Ref. [79].

In the case of matter NSIs, for a constant matter density profile (which is close to reality for most long-baseline neutrino oscillation experiments), the neutrino transition probabilities are given by

$$P(\nu_\alpha \to \nu_\beta; L) = \left|\sum_{i=1}^{3}\hat{U}_{\alpha i}\hat{U}^*_{\beta i}\,\mathrm{e}^{-\mathrm{i}\frac{\hat{m}^2_i L}{2E}}\right|^2 , \tag{16}$$

where L is the baseline length. Comparing Eq. (16) with the formula for neutrino transition probabilities in vacuum, one arrives at the conclusion that there is no difference between the form of the neutrino transition probabilities in matter with NSIs and in vacuum if one replaces the effective parameters $\hat{m}_i^2$ and $\hat{U}$ in Eq. (16) by the vacuum parameters m_i^2 and U. The mappings between the effective parameters and the vacuum ones are sufficient to study new physics effects entering future long-baseline neutrino oscillation experiments (see Section II B). The important point is the diagonalization of the effective Hamiltonian $\tilde{H}$ and the derivation of the explicit expressions for the effective parameters. Now, using Eq. (16), we can express the neutrino oscillation probabilities in matter with NSIs (for a realistic experiment) as follows [79]

$$P(\nu_\alpha \to \nu_\alpha; L) = 1 - 4 \sum_{i>j} |\hat{U}_{\alpha i} \hat{U}^*_{\alpha j}|^2 \sin^2 \left(\frac{\Delta \hat{m}^2_{ij} L}{4E} \right) , \tag{17}$$

$$P(\nu_\alpha \to \nu_\beta; L) = -4 \sum_{i>j} \mathrm{Re} \left(\hat{U}^*_{\alpha i} \hat{U}_{\beta i} \hat{U}_{\alpha j} \hat{U}^*_{\beta j} \right) \sin^2 \left(\frac{\Delta \hat{m}^2_{ij} L}{4E} \right) - 8 \mathcal{J} \prod_{i>j} \sin \left(\frac{\Delta \hat{m}^2_{ij} L}{4E} \right) \tag{18}$$

where (α, β) run over (e, μ), (μ, τ), and (τ, e) and the quantity $\mathcal{J}$ is defined through the relation

$$\begin{aligned} \mathcal{J}^2 = |\hat{U}_{\alpha i}|^2 |\hat{U}_{\beta j}|^2 |\hat{U}_{\alpha j}|^2 |\hat{U}_{\beta i}|^2 - \frac{1}{4} \Big(1 + |\hat{U}_{\alpha i}|^2 |\hat{U}_{\beta j}|^2 + |\hat{U}_{\alpha j}|^2 |\hat{U}_{\beta i}|^2 \\ - |\hat{U}_{\alpha i}|^2 - |\hat{U}_{\beta j}|^2 - |\hat{U}_{\alpha j}|^2 - |\hat{U}_{\beta i}|^2 \Big)^2 . \end{aligned} \tag{19}$$

C. Mappings with NSIs

In Ref. [79], model-independent mappings for the effective masses with NSIs during propagation processes, i.e., in matter, were derived, which are given by

$$\tilde{m}_1^2 \simeq \Delta m^2_{31} \left(\hat{A} + \alpha s^2_{12} + \hat{A} \varepsilon_{ee} \right) , \tag{20}$$

$$\tilde{m}_2^2 \simeq \Delta m^2_{31} \left[\alpha c^2_{12} - \hat{A} s^2_{23} \left(\varepsilon_{\mu\mu} - \varepsilon_{\tau\tau} \right) - \hat{A} s_{23} c_{23} \left(\varepsilon_{\mu\tau} + \varepsilon^*_{\mu\tau} \right) + \hat{A} \varepsilon_{\mu\mu} \right] , \tag{21}$$

$$\tilde{m}_3^2 \simeq \Delta m^2_{31} \left[1 + \hat{A} \varepsilon_{\tau\tau} + \hat{A} s^2_{23} \left(\varepsilon_{\mu\mu} - \varepsilon_{\tau\tau} \right) + \hat{A} s_{23} c_{23} \left(\varepsilon_{\mu\tau} + \varepsilon^*_{\mu\tau} \right) \right] , \tag{22}$$

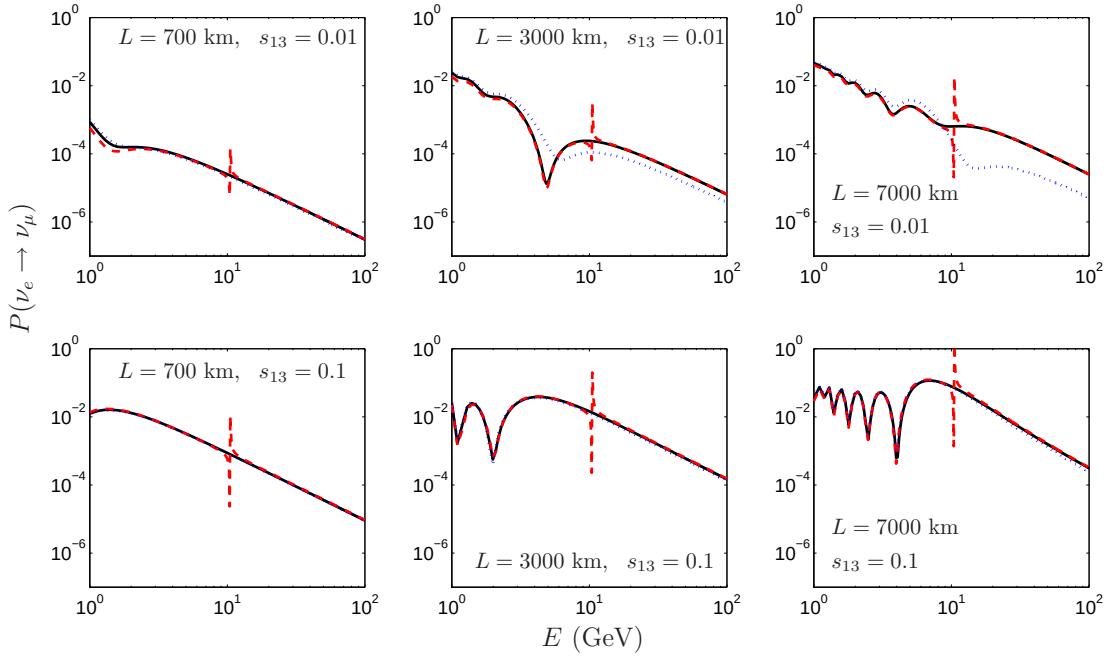

FIG. 2. Neutrino oscillation probabilities for the $\nu_e \to \nu_\mu$ channel as functions of the neutrino energy E. We have set $\delta = \pi/2$ and $\varepsilon_{e\tau} = 0.01$, and all other matter NSI parameters are zero. Solid (black) curves are exact numerical results, dashed (red) curves are the approximative results, and dotted (blue) curves are results without NSIs. This figure has been adopted from Ref. [79].

as well as model-independent mappings for the effective mixing matrix elements with NSIs, which are given by

$$\tilde{U}_{e3} \simeq \frac{s_{13}\mathrm{e}^{-\mathrm{i}\delta}}{1-\hat{A}} + \frac{\hat{A}(s_{23}\varepsilon_{e\mu} + c_{23}\varepsilon_{e\tau})}{1-\hat{A}}\,, \tag{23}$$

$$\tilde{U}_{e2} \simeq \frac{\alpha s_{12} c_{12}}{\hat{A}} + c_{23}\varepsilon_{e\mu} - s_{23}\varepsilon_{e\tau}\,, \tag{24}$$

$$\tilde{U}_{\mu 3} \simeq s_{23} + \hat{A}\left[c_{23}\varepsilon_{\mu\tau} + s_{23}c_{23}^2\left(\varepsilon_{\mu\mu} - \varepsilon_{\tau\tau}\right) - s_{23}^2 c_{23}\left(\varepsilon_{\mu\tau} + \varepsilon_{\mu\tau}^*\right)\right]\,, \tag{25}$$

where $\alpha \equiv \Delta m^2_{21}/\Delta m^2_{31}$ and $\hat{A} \equiv A/\Delta m^2_{31}$. We observe from the explicit mappings (20)–(25) that the effective parameters can be totally different from the fundamental parameters, because of the dependence on $\hat{A}$ and the NSI parameters $\varepsilon_{\alpha\beta}$. In addition, in Fig. 2, neutrino oscillation probabilities including the effects of NSIs for the electron neutrino-muon neutrino channel are plotted. It is found that the approximate mappings agree with the exact numerical results to an extremely good precision. Note that a singularity exists around 10 GeV due to the limitation of non-degenerate perturbation theory that has been used to derive the model-independent mappings.

D. Approximate formulas for two neutrino flavors

The three-flavor neutrino evolution given in Eq. (14) is rather complicated and cumbersome. Hence, in order to illuminate neutrino oscillations with NSIs, we investigate the oscillations using two flavors, e.g., ν_e and ν_τ. In this case, we have the much simpler two-flavor neutrino evolution equation

$$\mathrm{i}\frac{\mathrm{d}}{\mathrm{d}L}\begin{pmatrix}\nu_e\\ \nu_\tau\end{pmatrix} = \frac{1}{2E}\left[U\begin{pmatrix}0 & 0\\ 0 & \Delta m^2\end{pmatrix}U^\dagger + A\begin{pmatrix}1+\varepsilon_{ee} & \varepsilon_{e\tau}\\ \varepsilon_{e\tau} & \varepsilon_{\tau\tau}\end{pmatrix}\right]\begin{pmatrix}\nu_e\\ \nu_\tau\end{pmatrix}, \tag{26}$$

where L is the neutrino propagation length that has replaced time in Eq. (14). Using Eq. (26), one can derive the two-flavor neutrino oscillation probability

$$P(\nu_e \to \nu_\tau; L) = \sin^2(2\theta_M)\sin^2\left(\frac{\Delta m^2_M L}{2E}\right), \tag{27}$$

where θ_M and Δm^2_M are the effective neutrino oscillation parameters when taking into account NSIs. These parameters are related to the vacuum neutrino oscillation parameters θ and Δm^2 and given by (see e.g. Ref. [80])

$$\left(\Delta m^2_M\right)^2 = \left[\Delta m^2\cos(2\theta) - A\left(1+\varepsilon_{ee}-\varepsilon_{\tau\tau}\right)\right]^2 + \left[\Delta m^2\sin(2\theta) + 2A\varepsilon_{e\tau}\right]^2, \tag{28}$$

$$\sin(2\theta_M) = \frac{\Delta m^2\sin(2\theta) + 2A\varepsilon_{e\tau}}{\Delta m^2_M}. \tag{29}$$

For further discussion on approximate formulas for two neutrino flavors with NSIs, see Ref. [81].

IV. THEORETICAL MODELS FOR NSIS

In order to realize NSIs in a more fundamental framework with some underlying high-energy physics theory, it is generally desirable that it respects and encompasses the SM gauge group SU(3) × SU(2) × U(1). Note that the theoretical models presented in this section only represent a small selection, there exists many other models in the literature. In a toy model, including the SM and one heavy SU(2) singlet scalar field S, we can have the following interaction Lagrangian [82]

$$\mathcal{L}^S_{\mathrm{int}} = -\lambda_{\alpha\beta}\overline{L}^c_\alpha \mathrm{i}\sigma_2 L_\beta S, \tag{30}$$

where the quantities $\lambda_{\alpha\beta}$ $(\alpha, \beta = e, \mu, \tau)$ are elements of the coupling matrix λ, L_α is a doublet lepton field, and σ_2 is the second Pauli matrix. Now, integrating out the heavy field S, generates an anti-symmetric dimension-6 operator at tree level [83], i.e.,

$$\mathcal{L}_{\rm NSI}^{\rm d=6,as} = 4\frac{\lambda_{\alpha\beta}\lambda^*_{\delta\gamma}}{m_S^2}\left(\overline{\ell^c}_\alpha P_L \nu_\beta\right)\left(\bar{\nu}_\gamma P_R \ell^c_\delta\right) \,, \tag{31}$$

where m_S is the mass of the heavy field S as well as P_L and P_R are left- and right-handed projection operators, respectively. Note that this is the only dimension-6 operator, which does not give rise to charged-lepton NSIs.

A. Gauge symmetry invariance

At high-energy scales, where NSIs originate, there exists SU(2) × U(1) gauge symmetry invariance. In general, theories beyond the SM must respect gauge symmetry invariance, which implies strict constraints on possible models for NSIs (see e.g. Ref. [84]). Therefore, if there is a dimension-6 operator on the form

$$\frac{1}{\Lambda^2}\left(\bar{\nu}_\alpha \gamma^\rho P_L \nu_\beta\right)\left(\bar{\ell}_\gamma \gamma_\rho P_L \ell_\delta\right) \,,$$

then this operator will lead to NSI parameters such as $\varepsilon^{ee}_{e\mu}$. However, the above form for a dimension-6 operator must be a part of the more general form

$$\frac{1}{\Lambda^2}\left(\bar{L}_\alpha \gamma^\rho L_\beta\right)\left(\bar{L}_\gamma \gamma_\rho L_\delta\right) \,,$$

which involves four charged-lepton operators. Thus, we have severe constraints from experiments on processes like $\mu \to 3e$, i.e.,

$$\mathrm{BR}(\mu \to 3e) < 10^{-12} \,,$$

which leads to the following upper bound on the above chosen NSI parameter

$$\varepsilon^{ee}_{e\mu} < 10^{-6} \,.$$

Note that the above discussion is only valid for dimension-6 operators, and can be extended to operators with dimension equals to 8 or larger, but this will not be performed here.

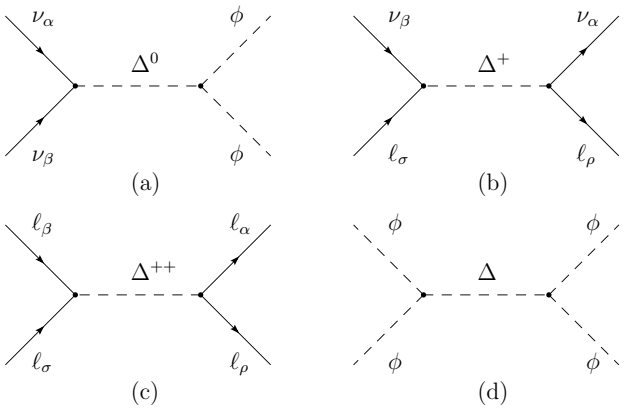

FIG. 3. Tree-level diagrams with exchange of a heavy triplet Higgs in the type-II seesaw model. This figure has been adopted from Ref. [85].

B. Different see-saw models

In a type-II seesaw model, the tree-level diagrams with exchange of a heavy triplet Higgs are given in Fig. 3. Integrating out the heavy triplet field (at tree level), we obtain the relations between the neutrino mass matrix and the NSI parameters as [85]

$$\varepsilon_{\alpha\beta}^{\rho\sigma} = -\frac{m_\Delta^2}{8\sqrt{2}G_F v^4 \lambda_\phi^2} (m_\nu)_{\sigma\beta} \left(m_\nu^\dagger\right)_{\alpha\rho} , \tag{32}$$

where $v \simeq 174$ GeV is the vacuum expectation value of the SM Higgs field, m_Δ is the mass of the Higgs triplet field, and λ_ϕ is associated with the trilinear Higgs coupling. Now, using experimental constraints from lepton flavor violations and rare decays, we find upper bounds on the NSI parameters, which are presented in Table II. From this table, we can observe that the NSI parameter $\varepsilon_{\mu e}^{\mu e}$ has the largest upper bound.

In addition, for $m_\Delta = 1\,\text{TeV}$ and varying m_1, we plot the upper bounds on some of the NSI parameters in the triplet seesaw model. The results are shown in Fig. 4. For a hierarchial mass spectrum (i.e., $m_1 < 0.05\,\text{eV}$), all the NSI effects are suppressed, whereas for a nearly degenerate mass spectrum (i.e., $m_1 > 0.1\,\text{eV}$), two NSI parameters can be sizable, which are $\varepsilon_{e\mu}^{e\mu}$ and ε_{ee}^{m}.

C. The Zee–Babu model

In the Zee–Babu model [86–88], we have the Lagrangian

$$\mathcal{L} = \mathcal{L}_{\text{SM}} + f_{\alpha\beta} L_{\text{L}\alpha}^T C \text{i}\sigma_2 L_{\text{L}\beta} h^+ + g_{\alpha\beta} \overline{e_\alpha^c} e_\beta k^{++} - \mu h^- h^- k^{++} + \text{h.c.} + V_H , \tag{33}$$

decay	constraint on	bound
$\mu^- \to e^- e^+ e^-$	$\lvert\varepsilon^{e\mu}_{ee}\rvert$	3.5×10^{-7}
$\tau^- \to e^- e^+ e^-$	$\lvert\varepsilon^{e\tau}_{ee}\rvert$	1.6×10^{-4}
$\tau^- \to \mu^- \mu^+ \mu^-$	$\lvert\varepsilon^{\mu\tau}_{\mu\mu}\rvert$	1.5×10^{-4}
$\tau^- \to e^- \mu^+ e^-$	$\lvert\varepsilon^{e\tau}_{e\mu}\rvert$	1.2×10^{-4}
$\tau^- \to \mu^- e^+ \mu^-$	$\lvert\varepsilon^{\mu\tau}_{\mu e}\rvert$	1.3×10^{-4}
$\tau^- \to e^- \mu^+ \mu^-$	$\lvert\varepsilon^{e\tau}_{\mu\mu}\rvert$	1.2×10^{-4}
$\tau^- \to e^- e^+ \mu^-$	$\lvert\varepsilon^{e\tau}_{\mu e}\rvert$	9.9×10^{-5}
$\mu^- \to e^- \gamma$	$\lvert\sum_\alpha \varepsilon^{e\mu}_{\alpha\alpha}\rvert$	1.4×10^{-4}
$\tau^- \to e^- \gamma$	$\lvert\sum_\alpha \varepsilon^{e\tau}_{\alpha\alpha}\rvert$	3.2×10^{-2}
$\tau^- \to \mu^- \gamma$	$\lvert\sum_\alpha \varepsilon^{\mu\tau}_{\alpha\alpha}\rvert$	2.5×10^{-2}
$\mu^+ e^- \to \mu^- e^+$	$\lvert\varepsilon^{\mu e}_{\mu e}\rvert$	3.0×10^{-3}

TABLE II. Constraints on various ε's from $\ell \to \ell\ell\ell$, one-loop $\ell \to \ell\gamma$, and $\mu^+ e^- \to \mu^- e^+$ processes.

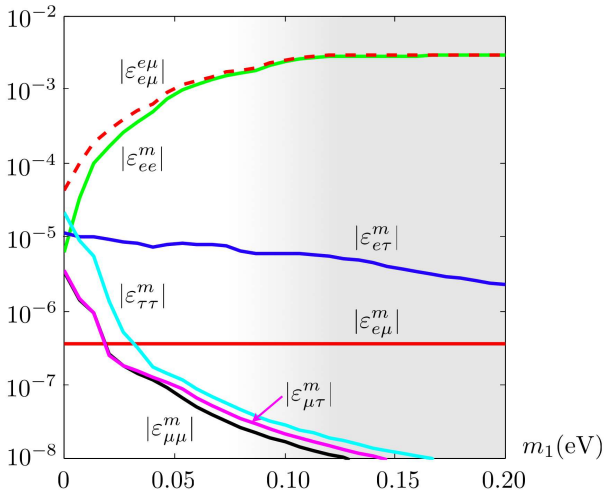

FIG. 4. Upper bounds on NSI parameters in the type-II seesaw model. This figure has been adopted from Ref. [85].

where h^+ and k^{++} are charged scalars that could be observed at the LHC and which lead to a two-loop diagram that generates small neutrino masses. The diagrams that are responsible for (a) NSIs of four charged leptons and (b) NSIs are presented in Fig. 5.

In Fig. 6, the allowed regions of the matter NSI parameters $\varepsilon_{\mu\mu}$ and $\varepsilon_{\tau\tau}$ in the Zee–Babu model are plotted. In the case of inverted neutrino mass hierarchy, the NSI parameters could

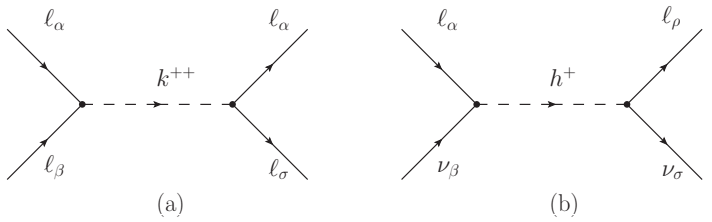

FIG. 5. Tree-level diagrams for the exchange of heavy scalars in the Zee–Babu model. This figure has been adopted from Ref. [89].

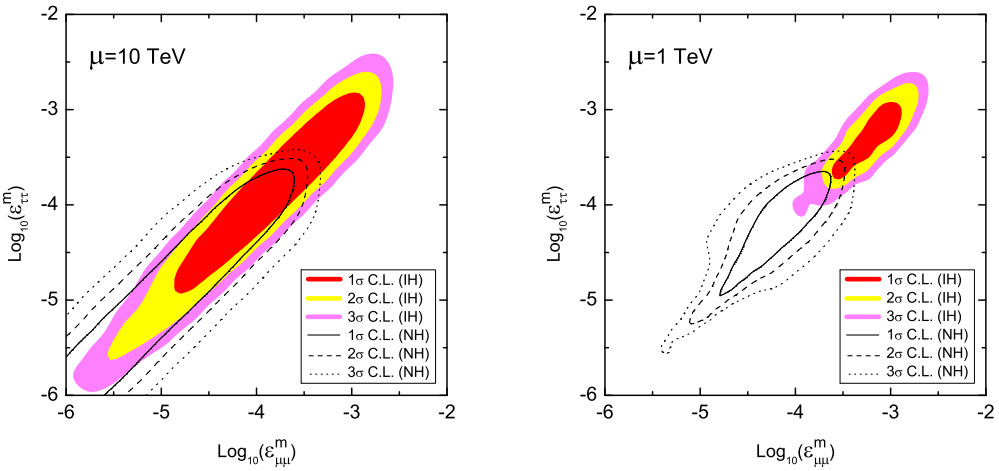

FIG. 6. The allowed region of NSI parameters at 1σ, 2σ, and 3σ C.L. in the Zee–Babu model. We take $m_h = m_k = \mu = 10$ TeV for the left plot and $m_h = m_k = \mu = 1$ TeV for the right plot. This figure has been adopted from Ref. [89].

be in the range $10^{-4} \div 10^{-3}$ [89].

V. PHENOMENOLOGY OF NSIS

In this section, we will discuss the phenomenology of NSIs for atmospheric, accelerator, and reactor neutrino experiments as well as for accelerators, neutrino factory setups, and astrophysical settings such as solar and supernova neutrinos. As we will see, only two experimental collaborations have used their neutrino data to analyze NSIs, which are the Super-Kamiokande and MINOS collaborations.

A. Atmospheric neutrino experiments

Neutrino oscillations with matter NSIs that are important for atmospheric neutrinos have been previously studied in the literature. For example, there are phenomenological studies that investigate the possibility to probe NSIs with atmospheric neutrino data only [90–92] and in combination with other neutrino data [93–98], whereas there exist also more theoretical investigations [81, 99]. However, most importantly, there is an experimental study on matter NSIs with atmospheric neutrino data from the Super-Kamiokande collaboration [100]. In principle, atmospheric neutrinos are very sensitive to matter NSIs, since they travel over long distances inside the Earth before being detected [97].

In order to analyze atmospheric neutrino data in the simplest way, we consider a two-flavor neutrino oscillation approximation with matter NSIs in the ν_μ-ν_τ sector (cf. Section III D), since $\nu_\mu \leftrightarrow \nu_\tau$ oscillations are important for atmospheric neutrinos. In this case, the first row and first column in Eq. (14) are cancelled, which effectively means that the NSI parameters that couple to ν_e are set to zero, i.e., $\varepsilon_{e\alpha} = 0$, where $\alpha = e, \mu, \tau$. In addition, the parameters Δm^2_{21}, θ_{12}, and θ_{13} are not important, leading to a two-flavor approximation that only includes the parameters $\Delta m^2 \equiv \Delta m^2_{31}$, $\theta \equiv \theta_{23}$, $\varepsilon_{\mu\mu}$, $\varepsilon_{\mu\tau} = \varepsilon_{\tau\mu}$, and $\varepsilon_{\tau\tau}$. In this approximation, which has been named the *two-flavor hybrid model*, the two-flavor neutrino evolution equation reads

$$\mathrm{i}\frac{\mathrm{d}}{\mathrm{d}L}\begin{pmatrix}\nu_\mu \\ \nu_\tau\end{pmatrix} = \frac{1}{2E}\left[U\begin{pmatrix}0 & 0 \\ 0 & \Delta m^2\end{pmatrix}U^\dagger + A\begin{pmatrix}1+\varepsilon_{\mu\mu} & \varepsilon_{\mu\tau} \\ \varepsilon_{\mu\tau} & \varepsilon_{\tau\tau}\end{pmatrix}\right]\begin{pmatrix}\nu_\mu \\ \nu_\tau\end{pmatrix} . \tag{34}$$

Using Eq. (34), defining $\varepsilon \equiv \varepsilon_{\mu\tau}$ and $\varepsilon' \equiv \varepsilon_{\tau\tau} - \varepsilon_{\mu\mu}$, and assuming that neutrinos have NSIs with d-quarks only [90, 101], we obtain the two-flavor ν_μ survival probability [91, 100]

$$P(\nu_\mu \to \nu_\mu; L) = 1 - P(\nu_\mu \to \nu_\tau; L) = 1 - \sin^2(2\Theta)\sin^2\left(\frac{\Delta m^2_{31} L}{4E} R\right) , \tag{35}$$

where the quantities Θ and R are given by

$$\sin^2(2\Theta) = \frac{1}{R^2}\left[\sin^2(2\theta) + R_0^2\sin^2(2\xi) + 2R_0\sin(2\theta)\sin(2\xi)\right] , \tag{36}$$

$$R = \sqrt{1 + R_0^2 + 2R_0\left[\cos(2\theta)\cos(2\xi) + \sin(2\theta)\sin(2\xi)\right]} \tag{37}$$

with the two auxiliary parameters

$$R_0 = \sqrt{2}G_F N_f \frac{4E}{\Delta m^2}\sqrt{|\varepsilon|^2 + \frac{\varepsilon'^2}{4}} , \tag{38}$$

$$\xi = \frac{1}{2}\arctan\left(\frac{2\varepsilon}{\varepsilon'}\right) . \tag{39}$$

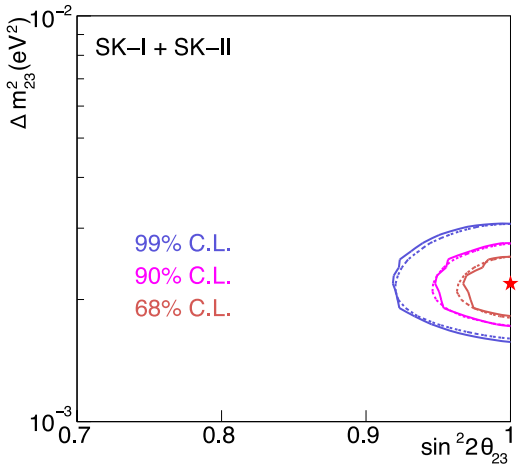

FIG. 7. Allowed parameter regions for $\sin^2(2\theta_{23})$ and Δm^2_{32} using the two-flavor hybrid model (solid curves) and standard two-flavor neutrino oscillations (dashed curves). The undisplayed parameters ε and ε' have been integrated out. This figure has been adopted from Ref. [100].

Now, using the two-flavor hybrid model together with atmospheric neutrino data from the Super-Kamiokande I (1996-2001) and II (2003-2005) experiments, the Super-Kamiokande collaboration has obtained the following results at 90 % C.L. [100]

$$|\varepsilon_{\mu\tau}| < 1.1 \cdot 10^{-2} \quad \text{and} \quad |\varepsilon_{\tau\tau} - \varepsilon_{\mu\mu}| < 4.9 \cdot 10^{-2}$$

and the allowed parameter regions for $\sin^2(2\theta_{23})$ and $\Delta m^2_{31} \simeq \Delta m^2_{32}$ with and without NSIs are shown in Fig. 7. In principle, there are no significant differences between the allowed parameters regions with NSIs and the ones without NSIs. This analysis can be extended to a similar analysis with a three-flavor hybrid model also taking into account the NSI parameters ε_{ee} and $\varepsilon_{e\tau}$, which, however, leads to no significant changes for the allowed values of the parameter regions compared to the two-flavor hybrid model. It should be noted that the atmospheric neutrino data have no possibility to constrain the NSI parameter ε_{ee} [95] and the other NSI parameter $\varepsilon_{e\tau}$ is related to both ε_{ee} and $\varepsilon_{\tau\tau}$ via the expression $\varepsilon_{\tau\tau} \sim 3|\varepsilon_{e\tau}|^2/(1+3\varepsilon_{ee})^2$ [92, 95, 100]. In conclusion, the Super-Kamiokande collaboration has found no evidence for matter NSIs in its atmospheric neutrino data.

B. Accelerator neutrino experiments

Studies of previous, present, and future setups of accelerator neutrino oscillation experiments including matter NSIs have been thoroughly investigated in the literature, especially

setups with long-baselines belong to these studies. Such studies include searches for matter NSIs with the K2K experiment [95], the MINOS experiment [80, 97, 99, 102–104], and the OPERA experiment [105–107], as well as sensitivity analyses of the NOνA experiment [108] and the T2K and T2KK experiments [109–111]. The prospects for detecting NSIs at the MiniBooNE experiment, which has a shorter baseline, has been investigated too [112, 113]. There are also studies that are more general in character [25, 98, 114]. In addition, the MINOS experiment has recently presented the results of a search for matter NSI in form of a poster at the "Neutrino 2012" conference in Kyoto, Japan [115].

Using three-flavor neutrino oscillations with matter NSIs for accelerator neutrinos, we will present the important NSI parameters and flavor transition probabilities for two experiments, which are (i) the MINOS experiment with baseline length $L \simeq 735$ km (from Fermilab in Illinois, USA to Soudan mine in Minnesota, USA) and neutrino energy in the interval $(1 \div 6)$ GeV and (ii) the OPERA experiment with baseline length $L \simeq 732$ km (from CERN in Geneva, Switzerland to LNGS in Gran Sasso, Italy) and average neutrino energy $E \simeq 17$ GeV. Note that the baseline lengths of the two experiments are nearly the same, but there is a difference in the neutrino energy, which is about one order of magnitude.

First, in the case of the MINOS experiment, the important NSI parameters are $\varepsilon_{e\tau}$ and $\varepsilon_{\tau\tau}$ [see Eq. (14)] and the interesting transition probability is the ν_μ survival probability (or equivalently the ν_μ disappearance probability), which to leading order is given by [103]

$$P(\nu_\mu \to \nu_\mu; L) \simeq 1 - \sin^2(2\tilde{\theta}_{23}) \sin^2\left(\frac{\Delta\tilde{m}^2_{31}}{4E} L\right) , \tag{40}$$

where three-flavor effects due to Δm^2_{21} and θ_{13} have been neglected, and the effective parameters are

$$\Delta\tilde{m}^2_{31} = \Delta m^2_{31} \xi \, , \tag{41}$$

$$\sin^2(2\tilde{\theta}_{23}) = \frac{\sin^2(2\theta_{23})}{\xi^2} \tag{42}$$

with

$$\xi = \sqrt{\left[\hat{A}\varepsilon_{\tau\tau} + \cos(2\theta_{23})\right]^2 + \sin^2(2\theta_{23})} \, . \tag{43}$$

Note that in Eqs. (41)–(43) we have used the NSI parameter $\varepsilon_{e\tau}$ as a perturbation and the formulas should hold if $|\varepsilon_{e\tau}|^2 A^2 L^2/(4E^2) \ll 1$ or, in the case of the MINOS experiment, if $|\varepsilon_{e\tau}| \ll 5.8$ [103]. Furthermore, it is possible to show the effective three-flavor mixing matrix

element $\hat{U}_{e3}$ is given by

$$\hat{U}_{e3} \simeq U_{e3} + \hat{A}\varepsilon_{e\tau}\cos(\theta_{23})\,, \tag{44}$$

which means that there could be a degeneracy between the mixing angle θ_{13} and the NSI parameter $\varepsilon_{e\tau}$ [103]. Now, since the mixing angle θ_{13} has been measured [116–119], the MINOS experiment can put a limit on $|\varepsilon_{e\tau}|$ [103]. In addition to the above discussion for the MINOS experiment, it has recently been argued in the literature that it should be possible to study the NSI parameter $\varepsilon_{\mu\tau}$ using the MINOS experiment too [97, 99, 104]. In this case (assuming $\theta_{23} = 45^\circ$), the ν_μ survival probability becomes [99]

$$P(\nu_\mu \to \nu_\mu; L) \simeq 1 - \sin^2\left(\left|\frac{\Delta m^2_{31}}{4E} - \varepsilon_{\mu\tau}\frac{A}{2E}\right| L\right)\,. \tag{45}$$

Now, using a model based on the ν_μ survival probability in Eq. (45) together with data from the MINOS experiment, the MINOS collaboration has obtained the following result for the matter NSI parameter $\varepsilon_{\mu\tau}$ at 90 % C.L. [115]

$$-0.200 < \varepsilon_{\mu\tau} < 0.070\,,$$

which means that MINOS has found no evidence for matter NSIs in its neutrino data, at least not a non-zero value for the matter NSI parameter $\varepsilon_{\mu\tau}$.

Second, in the case of the OPERA experiment, the important NSI parameter is $\varepsilon_{\mu\tau}$ [see Eq. (14)] due to the relatively short baseline length and the interesting transition probability is the appearance probability for oscillations of ν_μ into ν_τ, which is given by [107]

$$P(\nu_\mu \to \nu_\tau; L) = \left|c^2_{13}\sin(2\theta_{23})\frac{\Delta m^2_{31}}{4E} + \varepsilon^*_{\mu\tau}\frac{A}{2E}\right|^2 L^2 + \mathcal{O}(L^3)\,, \tag{46}$$

where it has been assumed that the small mass-squared difference $\Delta m^2_{21} = 0$. Thus, there exists a degeneracy between the fundamental neutrino oscillation parameters and the NSI parameter $\varepsilon_{\mu\tau}$. Note that it has been shown that the OPERA experiment is not very sensitive to the NSI parameters $\varepsilon_{e\tau}$ and $\varepsilon_{\tau\tau}$ [106].

C. Reactor neutrino experiments

To my knowledge, NSIs in reactor neutrino experiments have only been discussed in Refs. [66, 74, 120]. Below, we will summarize these three works.

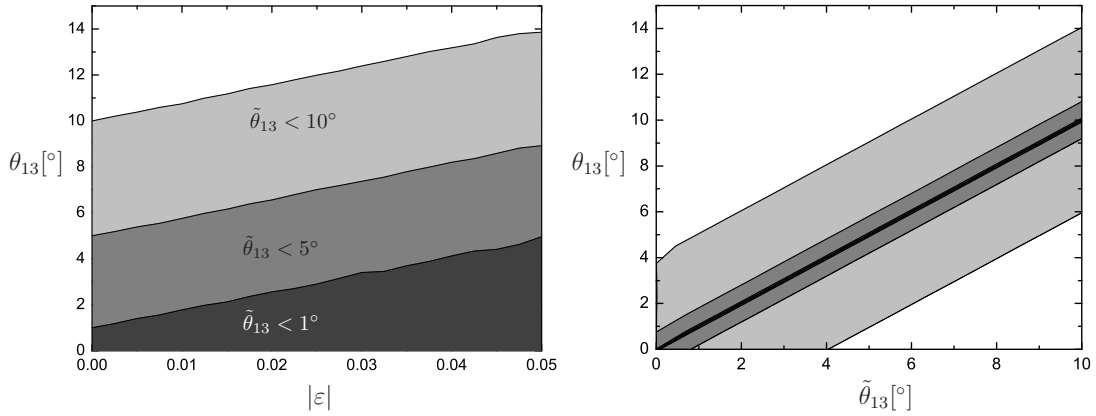

FIG. 8. Mappings among $\tilde{\theta}_{13}$, θ_{13}, and NSI parameters $\varepsilon_{\alpha\beta}$. This figure has been adopted from Ref. [74].

First, in Ref. [66], a combined study on the performance of reactor and superbeam neutrino experiments in the presence of NSIs is presented. Indeed, in this work, the authors argue that reactor and superbeam data can be used to establish the presence of NSIs.

Second, in Ref. [74], NSIs at reactor neutrino experiments only were studied. In Fig. 8, mappings among the effective mixing angle $\tilde{\theta}_{13}$, the fundamental mixing angle θ_{13}, and the NSI parameters $\varepsilon_{\alpha\beta}$ are plotted. Such plots could be important for the analyses of, for example, the Daya Bay, Double Chooz, and RENO experiments. It was found that (i) $\theta_{13} < 14°$, which is larger than the former CHOOZ bound that is about $10°$ and also larger than the recently measured values of the mixing angle θ_{13} and (ii) inspite of a very small θ_{13}, a sizable effective mixing angle can be achieved due to mimicking effects [74]. In principle, this means that the measured value for the mixing angle $\theta_{13} \approx 9°$ by the Daya Bay, Double Chooz, and RENO experiments [116–119] could be a combination of the fundamental value for θ_{13} (which should be smaller than the effective measured value) and effects of NSI parameters.

Third, in Ref. [120], NSIs at the Daya Bay experiment were studied. The authors of this work show that, under certain conditions, only three years of running of the Daya Bay experiment might be sufficient to provide a hint on NSIs. Thus, in future analyses of data from the Daya Bay experiment, it will be important to disentangle effects of NSI parameters on the mixing angle θ_{13} as well as the large neutrino mass-squared difference Δm^2_{31}. In Fig. 9, the effects of NSIs on θ_{13} and $\Delta m^2_{32} \simeq \Delta m^2_{31}$ are shown for Daya Bay after three years of running.

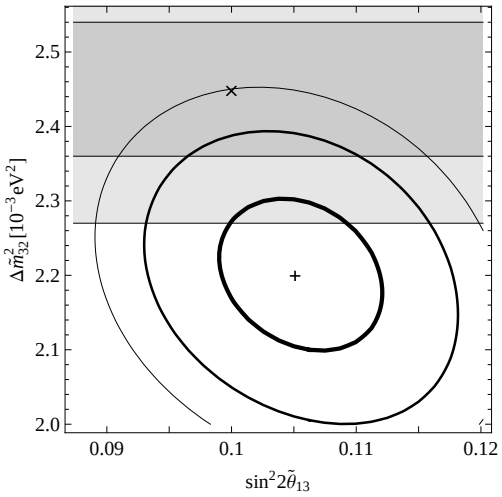

FIG. 9. Effects of NSIs on θ_{13} and Δm^2_{32} for Daya Bay after three years of running. This figure has been adopted from Ref. [120].

D. Accelerators

In Refs. [121, 122], the authors have explored an alternative approach to study NSIs by bringing into play collider data. Indeed, LEP provides bounds on NSIs of the order of $\varepsilon \lesssim (10^{-2} \div 10^{-3})$ at $\sqrt{s} \sim 200$ GeV, and if NSIs are contact interactions at LHC energies, LHC should have a sensitivity reach of NSIs of the order of $\varepsilon \gtrsim 3 \cdot 10^{-3}$ at 14 TeV and with 100 fb^{-1} of data. In addition, it should be mentioned that bounds on the NSI parameters ε^{qP}_{ee}, $\varepsilon^{qP}_{\tau\tau}$, and $\varepsilon^{qP}_{\tau e}$ ($q = u, d$ and $P = L, R$) have been derived [123], using 1 fb^{-1} data from the ATLAS experiment at LHC.

E. Neutrino Factory

Due to the large sensitivity at a future neutrino factory for small parameters such as NSI parameters, there exist a vast amount of investigations for different neutrino factory setups in connections to NSIs [58, 62, 65, 83, 85, 89, 93, 124–131]. In this section, we will present most of these investigations and what their general conclusions for NSIs at a future neutrino factory are. Several investigations have discussed the sensitivity and discovery reach of a neutrino factory in probing NSIs [93, 124–127, 131]. For example, it has been suggested that (i) a 100 GeV neutrino factory could probe flavor-changing neutrino interactions of the order of $|\varepsilon| \lesssim 10^{-4}$ at 99 % C.L. [93], (ii) there is an entanglement between the mixing angle θ_{13} and

NSI parameters,[1] which would be solved in the best way by using the appearance channel $\nu_e \to \nu_\mu$ [124, 125], (iii) there are degeneracies between CP violation and NSI parameters [130, 131], (iv) a neutrino factory has excellent prospects in detecting NSIs originating from "new physics" at the TeV scale [126], and (v) off-diagonal NSI parameters could be tested down to the order of 10^{-3}, whereas diagonal NSI parameter combinations such as $\varepsilon_{ee} - \varepsilon_{\tau\tau}$ and $\varepsilon_{\mu\mu} - \varepsilon_{\tau\tau}$ could only be tested down to 10^{-1} and 10^{-2}, respectively [131]. Furthermore, there are studies on the optimization of a neutrino factory with respect to NSI parameters, especially for $\varepsilon_{\mu\tau}$ and $\varepsilon_{\tau\tau}$ [128], as well as the impact of near detectors (with ν_τ detection) at a neutrino factory on NSIs [129]. In addition, it has been pointed out that the generation of matter NSIs might give rise to production and detection NSIs at a neutrino factory [83]. On the more theoretical side, some investigations on NSIs stemming from different models have been carried out. For example, NSIs from a triplet seesaw model [85] or the Zee–Babu model [89] have been investigated. At a neutrino factory, NSIs from the triplet seesaw model could lead to quite significant signals of lepton flavor violating decays, whereas production NSIs from the Zee–Babu model might be at an observable level in the $\nu_e \to \nu_\tau$ and/or $\nu_\mu \to \nu_\tau$ channels. Finally, it has been pointed out that NSIs and non-unitarity might phenomenologically lead to very similar effects for a neutrino factory, although for completely different reasons [65].

F. NSI effects on solar and supernova neutrino oscillations

In addition to studies on NSIs with atmospheric and man-made sources of neutrinos, there exist some investigations of NSI effects on solar and supernova neutrino oscillations [132–145]. First, we focus on NSIs with solar neutrinos, and then, we discuss NSIs with supernova neutrinos.

In the case of solar neutrinos, an analysis of data from the Super-Kamiokande and SNO experiments was performed to investigate the sensitivity of NSIs [133]. Furthermore, it has been suggested that the Borexino experiment can provide signatures for NSIs [133], and its data can also be used to place constraints on NSIs [140]. The LENA proposal has also been illustrated as a probe for NSIs [139]. In addition, non-universal flavor-conserving couplings

[1] This could be excluded due to the non-zero and quite large value for the mixing angle θ_{13} found by the Daya Bay, Double Chooz, and RENO collaborations [116–119].

with electrons, flavor-changing interactions, and NSIs in general can affect the phenomenology of solar neutrinos [132, 134–138].

In the case of supernova neutrinos, a three-flavor analysis for the possibility of probing NSIs, using neutrinos from a galactic supernova that propagate in the supernova envelope, has been performed [141]. Furthermore, the interplay between collective effects and NSIs for supernova neutrinos has been investigated [142–144]. Finally, a study on NSIs similar to Ref. [137] for solar neutrinos has been presented for supernova neutrinos by the same authors [145].

In addition to NSIs with solar and supernova neutrinos, other studies on NSIs with astrophysics have been carried out. For example, in Ref. [146], the authors investigate production and detection NSIs of high-energy neutrinos at neutrino telescopes, using neutrino flux ratios.

VI. PHENOMENOLOGICAL BOUNDS ON NSIS

As discussed above, there are basically two neutrino experiments that have put direct bounds on NSI parameters – the Super-Kamiokande and MINOS experiments (see Sections. V A and V B). However, there exist also some phenomenological works that have used different sets of data to find direct bounds on NSI parameters. Below, we will present direct bounds on both (i) matter NSIs and (ii) production and detection NSIs from such works. In addition, we will discuss NSIs for neutrino cross-sections.

A. Direct bounds on matter NSIs

In a work by Davidson *et al.* [62], bounds on matter NSI parameters using experiments with neutrinos and charged leptons have been derived for the realistic scenario with three flavors [62, 127, 147]

$$\begin{pmatrix} -0.9 < \varepsilon_{ee} < 0.75 & |\varepsilon_{e\mu}| \lesssim 3.8 \cdot 10^{-4} & |\varepsilon_{e\tau}| \lesssim 0.25 \\ & -0.05 < \varepsilon_{\mu\mu} < 0.08 & |\varepsilon_{\mu\tau}| \lesssim 0.25 \\ & & |\varepsilon_{\tau\tau}| \lesssim 0.4 \end{pmatrix} .$$

We observe that the bounds range from 10^{-4} to 1 for the different matter NSI parameters. Note that the bounds presented in this analysis are obtained using loop effects. However, it

turns out that bounds coming from loop effects are generally not applicable [148]. Therefore, in Ref. [148], Biggio, Blennow, and Fernández-Martínez have performed a new analysis. The result of this analysis is that the model-independent bound for the NSI parameter $\varepsilon_{e\mu}$ increases by a factor of 10^3. It should be noted that one-loop effects on NSIs have also been studied in Ref. [149]. Now, in Ref. [150], using bounds on NSI parameters from Refs. [62, 135, 151, 152], but disregarding the loop bound on the parameter $\varepsilon_{e\mu}^{fP}$, bounds on the effective matter NSI parameters have been estimated by Biggio, Blennow, and Fernández-Martínez. The model-independent bounds on the matter NSI parameters (for the Earth) are given by

$$\begin{pmatrix} |\varepsilon_{ee}| < 2.5 & |\varepsilon_{e\mu}| < 0.21 & |\varepsilon_{e\tau}| < 1.7 \\ & |\varepsilon_{\mu\mu}| < 0.046 & |\varepsilon_{\mu\tau}| < 0.21 \\ & & |\varepsilon_{\tau\tau}| < 9.0 \end{pmatrix} ,$$

which, except for the matter NSI parameters $\varepsilon_{\mu\mu}$ and $\varepsilon_{\mu\tau}$, are larger than the too stringent bounds found by Davidson *et al.* [62], and ranging between 10^{-2} and 10, i.e., they are one or two orders of magnitude larger than the previous bounds.

B. Direct bounds on production and detection NSIs

Finally, in Ref. [150], the authors have also derived model-independent bounds on production and detection NSIs. The most stringent bounds for charged-current-like NSIs for terrestrial experiments are the following

$$\begin{pmatrix} |\varepsilon_{ee}^{\mu e}| < 0.025 & |\varepsilon_{e\mu}^{\mu e}| < 0.030 & |\varepsilon_{e\tau}^{\mu e}| < 0.030 \\ |\varepsilon_{\mu e}^{\mu e}| < 0.025 & |\varepsilon_{\mu\mu}^{\mu e}| < 0.030 & |\varepsilon_{\mu\tau}^{\mu e}| < 0.030 \\ |\varepsilon_{\tau e}^{\mu e}| < 0.025 & |\varepsilon_{\tau\mu}^{\mu e}| < 0.030 & |\varepsilon_{\tau\tau}^{\mu e}| < 0.030 \end{pmatrix} ,$$

$$\begin{pmatrix} |\varepsilon_{ee}^{ud}| < 0.041 & |\varepsilon_{e\mu}^{ud}| < 0.025 & |\varepsilon_{e\tau}^{ud}| < 0.041 \\ |\varepsilon_{\mu e}^{ud}| < \begin{cases} 1.8 \cdot 10^{-6} \\ 0.026 \end{cases} & |\varepsilon_{\mu\mu}^{ud}| < 0.078 & |\varepsilon_{\mu\tau}^{ud}| < 0.013 \\ |\varepsilon_{\tau e}^{ud}| < \begin{cases} 0.087 \\ 0.12 \end{cases} & |\varepsilon_{\tau\mu}^{ud}| < \begin{cases} 0.013 \\ 0.018 \end{cases} & |\varepsilon_{\tau\tau}^{ud}| < 0.13 \end{pmatrix} ,$$

where, whenever two values are presented, the upper value refers to left-handed NSIs and the lower one to right-handed NSIs. These bounds are basically of the order of magnitude 10^{-2}.

C. NSIs for neutrino cross-sections

In this section, NSIs for neutrino cross-sections will be investigated in detail. Neutrino NSIs with either electrons or first generation quarks can be constrained by low-energy scattering data. In general, one finds that bounds are stringent for muon neutrino interactions, loose for electron neutrino interactions, and in principle, do not exist for tau neutrino interactions. Note that in the present overview of the upper bounds on the NSI parameters, the results from Biggio, Blennow, and Fernández-Martínez [150] have not been included.

The best measurement on electron neutrino-electron scattering comes from the LSND experiment, which found the cross-section of this process to be [153]

$$\sigma(\nu_e e \to \nu e) = (1.17 \pm 0.17) \frac{G_F^2 m_e E_\nu}{\pi} \,, \tag{47}$$

where m_e is the electron mass and E_ν is the neutrino energy, which should be compared with the SM cross-section $\sigma(\nu_e e \to \nu e)|_{\rm SM} \simeq 1.0967 G_F^2 m_e E_\nu/\pi$. Including NSIs, the expression for this cross-section becomes

$$\sigma(\nu_e e \to \nu e) = \frac{2 G_F^2 m_e E_\nu}{\pi} \left[(1 + g_L^e + \varepsilon_{ee}^{eL})^2 + \sum_{\alpha \neq e} |\varepsilon_{\alpha e}^{eL}|^2 + \frac{1}{3} (g_R^e + \varepsilon_{ee}^{eR})^2 + \frac{1}{3} \sum_{\alpha \neq e} |\varepsilon_{\alpha e}^{eR}|^2 \right] , \tag{48}$$

where $g_L^e \simeq -0.2718$ and $g_R^e \simeq 0.2326$. Using the LSND data and the NSI cross-section for electron neutrino-electron scattering, we obtain 90 % C.L. bounds on the NSI parameters (note that we are only considering one NSI parameter at a time) [62]

$$-0.07 < \varepsilon_{ee}^{eL} < 0.11 \,, \quad -1 < \varepsilon_{ee}^{eR} < 0.5$$

for flavor-conserving diagonal NSI parameters and

$$|\varepsilon_{\tau e}^{eL}| < 0.4 \,, \quad |\varepsilon_{\tau e}^{eR}| < 0.7$$

for flavor-changing NSI parameters. Considering both left- and right-handed diagonal NSIs, i.e., two NSI parameters simultaneously, a 90 % C.L. region between two ellipses is obtained

$$0.445 < (0.7282 + \varepsilon_{ee}^{eL})^2 + \frac{1}{3} (0.2326 + \varepsilon_{ee}^{eR})^2 < 0.725 \,,$$

which is shown in Fig. 10. Note that, in an update [154], more restrictive allowed 90 % C.L. bounds for the NSI parameters ε_{ee}^{eL} and ε_{ee}^{eR} have been found

$$-0.02 < \varepsilon_{ee}^{eL} < 0.09 \quad -0.11 < \varepsilon_{ee}^{eR} < 0.05 \,.$$

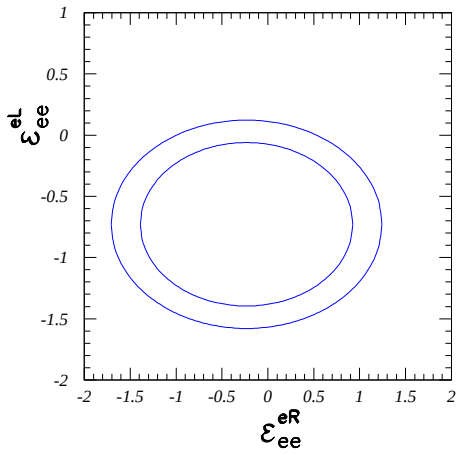

FIG. 10. Bounds on flavor-conserving NSIs of $\nu_e e$ scattering from the LSND experiment. This figure has been adopted from Ref. [62].

Then, we study electron neutrino-quark scattering. The CHARM collaboration [155] has measured the ratio between cross-sections and found

$$R^e = \frac{\sigma(\nu_e N \to \nu X) + \sigma(\bar{\nu}_e N \to \bar{\nu} X)}{\sigma(\nu_e N \to e X) + \sigma(\bar{\nu}_e N \to \bar{e} X)} = (\tilde{g}_{Le})^2 + (\tilde{g}_{Re})^2 = 0.406 \pm 0.140\,. \tag{49}$$

Including NSIs, the quantities $\tilde{g}_{Le}$ and $\tilde{g}_{Re}$ can be expressed as

$$(\tilde{g}_{Le})^2 = (g_L^u + \varepsilon_{ee}^{uL})^2 + \sum_{\alpha \neq e} |\varepsilon_{\alpha e}^{uL}|^2 + (g_L^d + \varepsilon_{ee}^{dL})^2 + \sum_{\alpha \neq e} |\varepsilon_{\alpha e}^{dL}|^2\,, \tag{50}$$

$$(\tilde{g}_{Re})^2 = (g_R^u + \varepsilon_{ee}^{uR})^2 + \sum_{\alpha \neq e} |\varepsilon_{\alpha e}^{uR}|^2 + (g_R^d + \varepsilon_{ee}^{dR})^2 + \sum_{\alpha \neq e} |\varepsilon_{\alpha e}^{dR}|^2\,. \tag{51}$$

Using the CHARM data, we obtain 90 % C.L. bounds on the NSI parameters (only one NSI parameter at a time) [62]

$$-1 < \varepsilon_{ee}^{uL} < 0.3\,, \quad -0.3 < \varepsilon_{ee}^{dL} < 0.3\,, \quad -0.4 < \varepsilon_{ee}^{uR} < 0.7\,, \quad -0.6 < \varepsilon_{ee}^{dR} < 0.5$$

for flavor-conserving NSIs and

$$|\varepsilon_{\tau e}^{qP}| < 0.5\,, \quad q = u, d \quad \text{and} \quad P = L, R$$

for flavor-changing NSIs. Again, a 90 % C.L. region considering several NSI parameters simultaneously can be obtained

$$0.176 < (0.3493 + \varepsilon_{ee}^{uL})^2 + (-0.4269 + \varepsilon_{ee}^{dL})^2 + (-0.1551 + \varepsilon_{ee}^{uR})^2 + (0.0775 + \varepsilon_{ee}^{dR})^2 < 0.636\,.$$

Next, for muon neutrino-electron scattering, the CHARM II collaboration [156] has measured $g_V^e = -0.035 \pm 0.017$ and $g_A^e = -0.503 \pm 0.017$, which translate into $g_L^e = -0.269 \pm 0.017$ and $g_R^e = 0.234 \pm 0.017$. Using these values, one can compute 90 % C.L. bounds on the NSI parameters (only one NSI parameter at a time) [62]

$$-0.025 < \varepsilon_{\mu\mu}^{eL} < 0.03\,, \quad -0.027 < \varepsilon_{\mu\mu}^{eR} < 0.03$$

for flavor diagonal NSIs and

$$|\varepsilon_{\tau\mu}^{eP}| < 0.1\,, \quad P = L, R$$

for flavor-changing NSIs. Furthermore, the NuTeV collaboration [157] has measured $(\tilde{g}_{L\mu})^2 = 0.3005 \pm 0.0014$ and $(\tilde{g}_{R\mu})^2 = 0.0310 \pm 0.0011$ that appear in ratios of cross-sections for neutrino-nucleon (muon neutrino-quark) scattering processes. Using these values, we obtain (only one NSI parameter at a time) [62]

$$\begin{aligned} -0.009 < \varepsilon_{\mu\mu}^{uL} < -0.003\,, \quad 0.002 < \varepsilon_{\mu\mu}^{dL} < 0.008\,, \\ -0.008 < \varepsilon_{\mu\mu}^{uR} < 0.003\,, \quad -0.008 < \varepsilon_{\mu\mu}^{dR} < 0.015 \end{aligned}$$

for flavor diagonal NSIs and

$$|\varepsilon_{\tau\mu}^{qR}| < 0.05\,, \quad q = u, d$$

for flavor-changing NSIs. Similarly, the 90 % C.L. regions using two NSI parameters simultaneously are presented in Fig. 11.

Finally, we investigate NSIs for the $e^+e^- \to \nu\bar{\nu}\gamma$ cross-section at LEP II. The 90 % C.L. bounds on flavor diagonal NSIs are given by [61]

$$-0.6 < \varepsilon_{\tau\tau}^{eL} < 0.4\,, \quad -0.4 < \varepsilon_{\tau\tau}^{eR} < 0.6\,,$$

whereas for flavor-changing NSIs

$$|\varepsilon_{\alpha\beta}^{eP}| < 0.4\,, \quad P = L, R, \quad \alpha = \tau, \quad \beta = e, \mu\,.$$

Also, for the NSI parameters $\varepsilon_{\tau\tau}^{eL}$ and $\varepsilon_{\tau\tau}^{eR}$, there exists an update [154] of the 90 % C.L. bounds

$$-0.51 < \varepsilon_{\tau\tau}^{eL} < 0.34 \quad -0.35 < \varepsilon_{\tau\tau}^{eR} < 0.50\,.$$

In conclusion, using neutrino cross-section measurements for the determination of upper bounds on NSIs, the only non-zero parameters obtained are $\varepsilon_{\mu\mu}^{uL}$ and $\varepsilon_{\mu\mu}^{dL}$. Therefore, for future analyses, new data on neutrino cross-sections would be valuable.

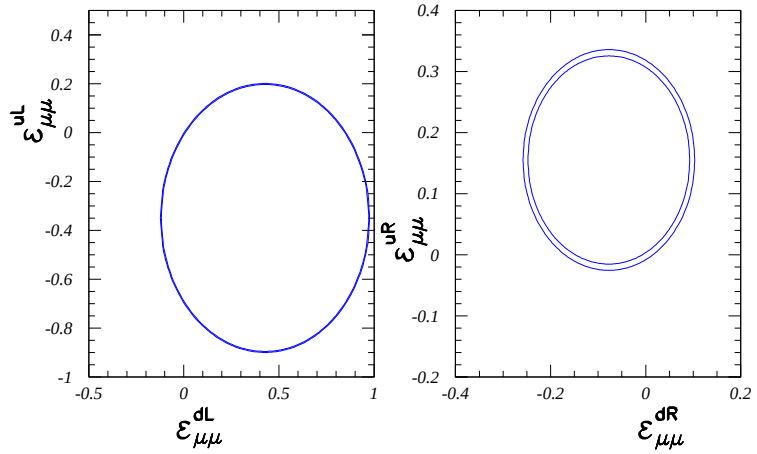

FIG. 11. Bounds on flavor-conserving NSIs of $\nu_\mu q$ scattering from the NuTeV experiment. This figure has been adopted from Ref. [62].

VII. SENSITIVITIES AND DISCOVERY REACH OF NSIS

I am sure that more investigations about NSIs will be conducted in the future, both theoretically and experimentally. In addition, I believe that a future neutrino factory[2] should be the most plausible experiment to find signatures of NSIs (see the detailed discussion in Section V E), but perhaps also the LHC will shed some light. The power of a neutrino factory is that it may have a sensitivity and discovery reach for the NSI parameters.

VIII. SUMMARY AND CONCLUSIONS

In summary of this review, we have discussed NSIs as sub-leading effects to the standard paradigm for neutrino flavor transitions based on the phenomenon of neutrino oscillations. Especially, we have presented both (i) production and detection NSIs including the so-called zero-distance effect as well as (ii) matter NSIs. In the case of matter NSIs, we have given approximate analytical model-independent mappings between effective neutrino masses and leptonic mixing angles and the fundamental neutrino mass-squared differences and leptonic mixing parameters. In addition, we have studied approximate two-flavor formulas for neutrino flavor transitions. Furthermore, we have presented some different theoretical models for

[2] Note that an interesting and important question is if a neutrino factory is going to be built or not, given a non-zero and quite large value for the mixing angle θ_{13}.

NSIs such as seesaw models and the Zee–Babu model, and investigated the phenomenology of NSIs in general. In particular, we have displayed the experimental results of upper bounds on NSIs from the analyses of the Super-Kamiokande ($|\varepsilon_{\mu\tau}| < 1.1 \cdot 10^{-2}, |\varepsilon_{\tau\tau} - \varepsilon_{\mu\mu}| < 4.9 \cdot 10^{-2}$) and MINOS ($-0.200 < \varepsilon_{\mu\tau} < 0.070$) collaborations, which both mean that no evidence for matter NSIs has been found. Moreover, we have indicated the sensitivities of NSIs for accelerators, a future neutrino factory, and the reactor neutrino experiment Daya Bay. For example, mimicking effects induced by NSIs could play a very important role in reactor neutrino experiments, especially for the mixing angle θ_{13}. In fact, the fundamental value for θ_{13} could be smaller than the measured value due to an interplay with NSIs. Finally, we have presented phenomenological upper bounds on NSIs. In the case of matter NSIs, former results gave bounds ranging from 10^{-4} to 1, whereas latter results yielded bounds between 10^{-2} and 10. In the case of production and detection NSIs for terrestrial experiments, there are bounds of the order from 10^{-6} to 0.1. In addition, we have given bounds for NSIs using data from neutrino cross-section measurements. Indeed, low-energy neutrino scattering experiments measuring neutrino cross-sections can be used to set bounds on NSI parameters. In conclusion, we have shortly discussed the future sensitivity and discovery reach of NSIs, which could be responsible for neutrino flavor transitions on a sub-leading level. Especially, the LHC and a future neutrino factory could open a new window towards determining the possible NSIs.

ACKNOWLEDGMENTS

I would like to thank Mattias Blennow and He Zhang for useful discussions and comments. This work was supported by the Swedish Research Council (Vetenskapsrådet), contract no. 621-2011-3985 (T.O.).

---

[1] Y. Fukuda *et al.* (Super-Kamiokande Collaboration), Phys. Rev. Lett. **81**, 1562 (1998), arXiv:hep-ex/9807003.

[2] T. Ohlsson, Nature **485**, 309 (2012).

[3] L. Wolfenstein, Phys. Rev. **D17**, 2369 (1978).

[4] S. Mikheyev and A. Y. Smirnov, Sov. J. Nucl. Phys. **42**, 913 (1985).

[5] T. Schwetz, "Review on global fits," (2012), talk presented at the workshop "What's ν?: From new experimental neutrino results to a deep understanding of theoretical physics and cosmology", Florence, Italy, June 25, 2012.

[6] D. Forero, M. Tórtola, and J. Valle, (2012), arXiv:1205.4018 [hep-ph].

[7] G. Fogli, E. Lisi, A. Marrone, D. Montanino, A. Palazzo, *et al.*, Phys. Rev. **D86**, 013012 (2012), arXiv:1205.5254 [hep-ph].

[8] Q. R. Ahmad *et al.* (SNO Collaboration), Phys. Rev. Lett. **87**, 071301 (2001), arXiv:nucl-ex/0106015.

[9] K. Eguchi *et al.* (KamLAND Collaboration), Phys. Rev. Lett. **90**, 021802 (2003), arXiv:hep-ex/0212021.

[10] M. Blennow, T. Ohlsson, and W. Winter, JHEP **06**, 049 (2005), arXiv:hep-ph/0502147.

[11] Y. Grossman and M. P. Worah, (1998), arXiv:hep-ph/9807511.

[12] E. Lisi, A. Marrone, and D. Montanino, Phys. Rev. Lett. **85**, 1166 (2000), arXiv:hep-ph/0002053.

[13] S. L. Adler, Phys. Rev. **D62**, 117901 (2000), arXiv:hep-ph/0005220.

[14] A. Gago, E. Santos, W. Teves, and R. Zukanovich Funchal, Phys. Rev. **D63**, 073001 (2001), arXiv:hep-ph/0009222.

[15] A. Gago, E. Santos, W. Teves, and R. Zukanovich Funchal, Phys. Rev. **D63**, 113013 (2001), arXiv:hep-ph/0010092.

[16] T. Ohlsson, Phys. Lett. **B502**, 159 (2001), arXiv:hep-ph/0012272.

[17] A. Gago, E. Santos, W. Teves, and R. Zukanovich Funchal, (2002), arXiv:hep-ph/0208166.

[18] G. Fogli, E. Lisi, A. Marrone, and D. Montanino, Phys. Rev. **D67**, 093006 (2003), arXiv:hep-ph/0303064.

[19] G. Barenboim and N. E. Mavromatos, JHEP **0501**, 034 (2005), arXiv:hep-ph/0404014.

[20] D. Morgan, E. Winstanley, J. Brunner, and L. F. Thompson, Astropart. Phys. **25**, 311 (2006), arXiv:astro-ph/0412618.

[21] L. A. Anchordoqui, H. Goldberg, M. Gonzalez-Garcia, F. Halzen, D. Hooper, *et al.*, Phys. Rev. **D72**, 065019 (2005), arXiv:hep-ph/0506168.

[22] G. Barenboim, N. E. Mavromatos, S. Sarkar, and A. Waldron-Lauda, Nucl. Phys. **B758**, 90 (2006), arXiv:hep-ph/0603028.

[23] G. Fogli, E. Lisi, A. Marrone, D. Montanino, and A. Palazzo, Phys. Rev. **D76**, 033006 (2007), arXiv:0704.2568 [hep-ph].

[24] J. Alexandre, K. Farakos, N. Mavromatos, and P. Pasipoularides, Phys. Rev. **D77**, 105001 (2008), arXiv:0712.1779 [hep-ph].

[25] N. C. Ribeiro, H. Nunokawa, T. Kajita, S. Nakayama, P. Ko, *et al.*, Phys. Rev. **D77**, 073007 (2008), arXiv:0712.4314 [hep-ph].

[26] N. E. Mavromatos, A. Meregaglia, A. Rubbia, A. Sakharov, and S. Sarkar, Phys. Rev. **D77**, 053014 (2008), arXiv:0801.0872 [hep-ph].

[27] Y. Farzan, T. Schwetz, and A. Y. Smirnov, JHEP **0807**, 067 (2008), arXiv:0805.2098 [hep-ph].

[28] J. N. Bahcall, N. Cabibbo, and A. Yahil, Phys. Rev. Lett. **28**, 316 (1972).

[29] V. D. Barger, W.-Y. Keung, and S. Pakvasa, Phys. Rev. **D25**, 907 (1982).

[30] J. Valle, Phys. Lett. **B131**, 87 (1983).

[31] V. D. Barger, J. Learned, S. Pakvasa, and T. J. Weiler, Phys. Rev. Lett. **82**, 2640 (1999), arXiv:astro-ph/9810121.

[32] S. Choubey and S. Goswami, Astropart. Phys. **14**, 67 (2000), arXiv:hep-ph/9904257.

[33] V. D. Barger, J. Learned, P. Lipari, M. Lusignoli, S. Pakvasa, *et al.*, Phys. Lett. **B462**, 109 (1999), arXiv:hep-ph/9907421.

[34] G. L. Fogli, E. Lisi, A. Marrone, and G. Scioscia, Phys. Rev. **D59**, 117303 (1999), arXiv:hep-ph/9902267.

[35] S. Pakvasa, AIP Conf. Proc. **542**, 99 (2000), arXiv:hep-ph/0004077.

[36] S. Choubey, S. Goswami, and D. Majumdar, Phys. Lett. **B484**, 73 (2000), arXiv:hep-ph/0004193.

[37] A. Bandyopadhyay, S. Choubey, and S. Goswami, Phys. Rev. **D63**, 113019 (2001), arXiv:hep-ph/0101273.

[38] M. Lindner, T. Ohlsson, and W. Winter, Nucl. Phys. **B607**, 326 (2001), arXiv:hep-ph/0103170.

[39] M. Lindner, T. Ohlsson, and W. Winter, Nucl. Phys. **B622**, 429 (2002), arXiv:astro-ph/0105309.

[40] A. S. Joshipura, E. Masso, and S. Mohanty, Phys. Rev. **D66**, 113008 (2002), arXiv:hep-ph/0203181.

[41] J. F. Beacom and N. F. Bell, Phys. Rev. **D65**, 113009 (2002), arXiv:hep-ph/0204111.

[42] A. Bandyopadhyay, S. Choubey, and S. Goswami, Phys. Lett. **B555**, 33 (2003), arXiv:hep-ph/0204173.

[43] J. F. Beacom, N. F. Bell, D. Hooper, S. Pakvasa, and T. J. Weiler, Phys. Rev. Lett. **90**, 181301 (2003), arXiv:hep-ph/0211305.

[44] D. Indumathi, (2002), arXiv:hep-ph/0212038.

[45] S. Ando, Phys. Lett. **B570**, 11 (2003), arXiv:hep-ph/0307169.

[46] G. Fogli, E. Lisi, A. Mirizzi, and D. Montanino, Phys. Rev. **D70**, 013001 (2004), arXiv:hep-ph/0401227.

[47] S. Ando, Phys. Rev. **D70**, 033004 (2004), arXiv:hep-ph/0405200.

[48] S. Palomares-Ruiz, S. Pascoli, and T. Schwetz, JHEP **0509**, 048 (2005), arXiv:hep-ph/0505216.

[49] D. Meloni and T. Ohlsson, Phys. Rev. **D75**, 125017 (2007), arXiv:hep-ph/0612279.

[50] M. Gonzalez-Garcia and M. Maltoni, Phys. Lett. **B663**, 405 (2008), arXiv:0802.3699 [hep-ph].

[51] M. Maltoni and W. Winter, JHEP **0807**, 064 (2008), arXiv:0803.2050 [hep-ph].

[52] P. Mehta and W. Winter, JCAP **1103**, 041 (2011), arXiv:1101.2673 [hep-ph].

[53] P. Baerwald, M. Bustamante, and W. Winter, (2012), arXiv:1208.4600 [astro-ph.CO].

[54] Y. Ashie *et al.* (Super-Kamiokande Collaboration), Phys. Rev. Lett. **93**, 101801 (2004), arXiv:hep-ex/0404034.

[55] T. Araki *et al.* (KamLAND Collaboration), Phys. Rev. Lett. **94**, 081801 (2005), arXiv:hep-ex/0406035.

[56] P. Adamson *et al.* (MINOS Collaboration), Phys. Rev. Lett. **101**, 131802 (2008), arXiv:0806.2237 [hep-ex].

[57] P. Adamson *et al.* (MINOS Collaboration), Phys. Rev. Lett. **106**, 181801 (2011), arXiv:1103.0340 [hep-ex].

[58] M. Blennow, T. Ohlsson, and W. Winter, Eur. Phys. J. **C49**, 1023 (2007), arXiv:hep-ph/0508175.

[59] S. Mikheyev and A. Y. Smirnov, Nuovo Cim. **C9**, 17 (1986).

[60] Y. Grossman, Phys. Lett. **B359**, 141 (1995), arXiv:hep-ph/9507344.

[61] Z. Berezhiani and A. Rossi, Phys. Lett. **B535**, 207 (2002), arXiv:hep-ph/0111137.

[62] S. Davidson, C. Peña-Garay, N. Rius, and A. Santamaria, JHEP **03**, 011 (2003), arXiv:hep-ph/0302093.

[63] M. Gonzalez-Garcia, Y. Grossman, A. Gusso, and Y. Nir, Phys. Rev. **D64**, 096006 (2001), arXiv:hep-ph/0105159.

[64] S. M. Bilenky and C. Giunti, Phys. Lett. **B300**, 137 (1993), arXiv:hep-ph/9211269.

[65] D. Meloni, T. Ohlsson, W. Winter, and H. Zhang, JHEP **1004**, 041 (2010), arXiv:0912.2735 [hep-ph].

[66] J. Kopp, M. Lindner, T. Ota, and J. Sato, Phys. Rev. **D77**, 013007 (2008), arXiv:0708.0152 [hep-ph].

[67] Z.-z. Xing, Int. J. Mod. Phys. **A23**, 4255 (2008), arXiv:0810.1421 [hep-ph].

[68] S. Antusch, C. Biggio, E. Fernández-Martínez, M. Gavela, and J. López-Pavón, JHEP **0610**, 084 (2006), arXiv:hep-ph/0607020.

[69] E. Fernández-Martínez, M. Gavela, J. López-Pavón, and O. Yasuda, Phys. Lett. **B649**, 427 (2007), arXiv:hep-ph/0703098.

[70] S. Goswami and T. Ota, Phys. Rev. **D78**, 033012 (2008), arXiv:0802.1434 [hep-ph].

[71] Z.-z. Xing and S. Zhou, Phys. Lett. **B666**, 166 (2008), arXiv:0804.3512 [hep-ph].

[72] S. Luo, Phys. Rev. **D78**, 016006 (2008), arXiv:0804.4897 [hep-ph].

[73] G. Altarelli and D. Meloni, Nucl. Phys. **B809**, 158 (2009), arXiv:0809.1041 [hep-ph].

[74] T. Ohlsson and H. Zhang, Phys. Lett. **B671**, 99 (2009), arXiv:0809.4835 [hep-ph].

[75] P. Langacker and D. London, Phys. Rev. **D38**, 907 (1988).

[76] J. Valle, Phys. Lett. **B199**, 432 (1987).

[77] M. Guzzo, A. Masiero, and S. Petcov, Phys. Lett. **B260**, 154 (1991).

[78] E. Roulet, Phys. Rev. **D44**, 935 (1991).

[79] D. Meloni, T. Ohlsson, and H. Zhang, JHEP **04**, 033 (2009), arXiv:0901.1784 [hep-ph].

[80] N. Kitazawa, H. Sugiyama, and O. Yasuda, (2006), arXiv:hep-ph/0606013.

[81] M. Blennow and T. Ohlsson, Phys. Rev. **D78**, 093002 (2008), arXiv:0805.2301 [hep-ph].

[82] M. S. Bilenky and A. Santamaria, Nucl. Phys. **B420**, 47 (1994), arXiv:hep-ph/9310302.

[83] S. Antusch, J. P. Baumann, and E. Fernández-Martínez, Nucl. Phys. **B810**, 369 (2009), arXiv:0807.1003 [hep-ph].

[84] D. Hernandez, (2009), arXiv:0911.4764 [hep-ph].

[85] M. Malinský, T. Ohlsson, and H. Zhang, Phys. Rev. **D79**, 011301(R) (2009), arXiv:0811.3346 [hep-ph].

[86] A. Zee, Phys. Lett. **B161**, 141 (1985).

[87] A. Zee, Nucl. Phys. **B264**, 99 (1986).

[88] K. S. Babu, Phys. Lett. **B203**, 132 (1988).

[89] T. Ohlsson, T. Schwetz, and H. Zhang, Phys. Lett. **B681**, 269 (2009), arXiv:0909.0455 [hep-ph].

[90] N. Fornengo, M. Maltoni, R. Tomàs, and J. Valle, Phys. Rev. **D65**, 013010 (2002), arXiv:hep-ph/0108043.

[91] M. Gonzalez-Garcia and M. Maltoni, Phys. Rev. **D70**, 033010 (2004), arXiv:hep-ph/0404085.

[92] A. Friedland, C. Lunardini, and M. Maltoni, Phys. Rev. **D70**, 111301 (2004), arXiv:hep-ph/0408264.

[93] P. Huber and J. Valle, Phys. Lett. **B523**, 151 (2001), arXiv:hep-ph/0108193.

[94] M. Guzzo, P. de Holanda, M. Maltoni, H. Nunokawa, M. Tórtola, *et al.*, Nucl. Phys. **B629**, 479 (2002), arXiv:hep-ph/0112310.

[95] A. Friedland and C. Lunardini, Phys. Rev. **D72**, 053009 (2005), arXiv:hep-ph/0506143.

[96] M. Gonzalez-Garcia, M. Maltoni, and J. Salvado, JHEP **1105**, 075 (2011), arXiv:1103.4365 [hep-ph].

[97] J. Kopp, P. A. Machado, and S. J. Parke, Phys. Rev. **D82**, 113002 (2010), arXiv:1009.0014 [hep-ph].

[98] F. Escrihuela, M. Tórtola, J. Valle, and O. Miranda, Phys. Rev. **D83**, 093002 (2011), arXiv:1103.1366 [hep-ph].

[99] W. A. Mann, D. Cherdack, W. Musial, and T. Kafka, Phys. Rev. **D82**, 113010 (2010), arXiv:1006.5720 [hep-ph].

[100] G. Mitsuka *et al.* (Super-Kamiokande Collaboration), Phys. Rev. **D84**, 113008 (2011), arXiv:1109.1889 [hep-ex].

[101] M. Gonzalez-Garcia, M. Guzzo, P. Krastev, H. Nunokawa, O. Peres, *et al.*, Phys. Rev. Lett. **82**, 3202 (1999), arXiv:hep-ph/9809531.

[102] A. Friedland and C. Lunardini, Phys. Rev. **D74**, 033012 (2006), arXiv:hep-ph/0606101.

[103] M. Blennow, T. Ohlsson, and J. Skrotzki, Phys. Lett. **B660**, 522 (2008), arXiv:hep-ph/0702059.

[104] Z. Isvan (MINOS Collaboration), (2011), arXiv:1110.1900 [hep-ex].

[105] T. Ota and J. Sato, Phys. Lett. **B545**, 367 (2002), arXiv:hep-ph/0202145.

[106] A. Esteban-Pretel, J. Valle, and P. Huber, Phys. Lett. **B668**, 197 (2008), arXiv:0803.1790 [hep-ph].

[107] M. Blennow, D. Meloni, T. Ohlsson, F. Terranova, and M. Westerberg, Eur. Phys. J. **C56**, 529 (2008), arXiv:0804.2744 [hep-ph].

[108] A. Friedland and I. M. Shoemaker, (2012), arXiv:1207.6642 [hep-ph].

[109] H. Oki and O. Yasuda, Phys. Rev. **D82**, 073009 (2010), arXiv:1003.5554 [hep-ph].

[110] O. Yasuda, Nucl. Phys. Proc. Suppl. **217**, 220 (2011), arXiv:1011.6440 [hep-ph].

[111] R. Adhikari, S. Chakraborty, A. Dasgupta, and S. Roy, (2012), arXiv:1201.3047 [hep-ph].

[112] L. M. Johnson, R. S. Williams, L. F. Spencer, and B. J. DeWilde, (2006), arXiv:hep-ph/0610011.

[113] E. Akhmedov and T. Schwetz, JHEP **1010**, 115 (2010), arXiv:1007.4171 [hep-ph].

[114] T. Ota, J. Sato, and N.-a. Yamashita, Phys. Rev. **D65**, 093015 (2002), arXiv:hep-ph/0112329.

[115] J. A. B. Coelho (MINOS Collaboration), "Search for effects of exotic models in MINOS," (2012), poster presented at the XXVth International Conference on Neutrino Physics & Astrophysics (Neutrino 2012), Kyoto, Japan, June 3-9, 2012.

[116] F. An *et al.* (Daya Bay Collaboration), Phys. Rev. Lett. **108**, 171803 (2012), arXiv:1203.1669 [hep-ex].

[117] Y. Abe *et al.* (Double Chooz Collaboration), Phys. Rev. Lett. **108**, 131801 (2012), arXiv:1112.6353 [hep-ex].

[118] Y. Abe *et al.* (Double Chooz Collaboration), (2012), arXiv:1207.6632 [hep-ex].

[119] J. Ahn *et al.* (RENO collaboration), Phys. Rev. Lett. **108**, 191802 (2012), arXiv:1204.0626 [hep-ex].

[120] R. Leitner, M. Malinský, B. Roskovec, and H. Zhang, JHEP **1112**, 001 (2011), arXiv:1105.5580 [hep-ph].

[121] S. Davidson and V. Sanz, Phys. Rev. **D84**, 113011 (2011), arXiv:1108.5320 [hep-ph].

[122] S. Davidson and V. Sanz, (2011), arXiv:1110.1558 [hep-ph].

[123] A. Friedland, M. L. Graesser, I. M. Shoemaker, and L. Vecchi, Phys. Lett. **B714**, 267 (2012), arXiv:1111.5331 [hep-ph].

[124] P. Huber, T. Schwetz, and J. Valle, Phys. Rev. Lett. **88**, 101804 (2002), arXiv:hep-ph/0111224.

[125] P. Huber, T. Schwetz, and J. Valle, Phys. Rev. **D66**, 013006 (2002), arXiv:hep-ph/0202048.

[126] J. Kopp, M. Lindner, and T. Ota, Phys. Rev. **D76**, 013001 (2007), arXiv:hep-ph/0702269.

[127] N. Ribeiro, H. Minakata, H. Nunokawa, S. Uchinami, and R. Zukanovich-Funchal, JHEP **0712**, 002 (2007), arXiv:0709.1980 [hep-ph].

[128] J. Kopp, T. Ota, and W. Winter, Phys. Rev. **D78**, 053007 (2008), arXiv:0804.2261 [hep-ph].

[129] J. Tang and W. Winter, Phys. Rev. **D80**, 053001 (2009), arXiv:0903.3039 [hep-ph].

[130] A. Gago, H. Minakata, H. Nunokawa, S. Uchinami, and R. Zukanovich Funchal, JHEP **1001**, 049 (2010), arXiv:0904.3360 [hep-ph].

[131] P. Coloma, A. Donini, J. López-Pavón, and H. Minakata, JHEP **1108**, 036 (2011), arXiv:1105.5936 [hep-ph].

[132] S. Bergmann, M. Guzzo, P. de Holanda, P. Krastev, and H. Nunokawa, Phys. Rev. **D62**, 073001 (2000), arXiv:hep-ph/0004049.

[133] Z. Berezhiani, R. Raghavan, and A. Rossi, Nucl. Phys. **B638**, 62 (2002), arXiv:hep-ph/0111138.

[134] M. Guzzo, P. de Holanda, and O. Peres, Phys. Lett. **B591**, 1 (2004), arXiv:hep-ph/0403134.

[135] A. Bolaños, O. Miranda, A. Palazzo, M. Tórtola, and J. Valle, Phys. Rev. **D79**, 113012 (2009), arXiv:0812.4417 [hep-ph].

[136] A. Palazzo and J. Valle, Phys. Rev. **D80**, 091301 (2009), arXiv:0909.1535 [hep-ph].

[137] C. Das and J. Pulido, Phys. Rev. **D83**, 053009 (2011), arXiv:1007.2167 [hep-ph].

[138] A. Palazzo, Phys. Rev. **D83**, 101701 (2011), arXiv:1101.3875 [hep-ph].

[139] E. Garcés, O. Miranda, M. Tórtola, and J. Valle, Phys. Rev. **D85**, 073006 (2012), arXiv:1112.3633 [hep-ph].

[140] S. K. Agarwalla, F. Lombardi, and T. Takeuchi, (2012), arXiv:1207.3492 [hep-ph].

[141] A. Esteban-Pretel, R. Tomàs, and J. Valle, Phys. Rev. **D76**, 053001 (2007), arXiv:0704.0032 [hep-ph].

[142] M. Blennow, A. Mirizzi, and P. D. Serpico, Phys. Rev. **D78**, 113004 (2008), arXiv:0810.2297 [hep-ph].

[143] A. Esteban-Pretel, R. Tomàs, and J. Valle, Phys. Rev. **D81**, 063003 (2010), arXiv:0909.2196 [hep-ph].

[144] B. Dasgupta, G. G. Raffelt, and I. Tamborra, Phys. Rev. **D81**, 073004 (2010), arXiv:1001.5396 [hep-ph].

[145] C. Das and J. Pulido, (2011), arXiv:1111.6939 [hep-ph].

[146] M. Blennow and D. Meloni, Phys. Rev. **D80**, 065009 (2009), arXiv:0901.2110 [hep-ph].

[147] J. Abdallah *et al.* (DELPHI Collaboration), Eur. Phys. J. **C38**, 395 (2005), arXiv:hep-ex/0406019.

[148] C. Biggio, M. Blennow, and E. Fernández-Martínez, JHEP **03**, 139 (2009), arXiv:0902.0607 [hep-ph].

[149] B. Bellazzini, Y. Grossman, I. Nachshon, and P. Paradisi, JHEP **1106**, 104 (2011), arXiv:1012.3759 [hep-ph].

[150] C. Biggio, M. Blennow, and E. Fernández-Martínez, JHEP **08**, 090 (2009), arXiv:0907.0097 [hep-ph].

[151] J. Barranco, O. Miranda, C. Moura, and J. Valle, Phys. Rev. **D73**, 113001 (2006), arXiv:hep-ph/0512195.

[152] J. Barranco, O. Miranda, C. Moura, and J. Valle, Phys. Rev. **D77**, 093014 (2008), arXiv:0711.0698 [hep-ph].

[153] L. B. Auerbach *et al.* (LSND Collaboration), Phys. Rev. **D63**, 112001 (2001), arXiv:hep-ex/0101039.

[154] D. Forero and M. Guzzo, Phys. Rev. **D84**, 013002 (2011).

[155] J. Dorenbosch *et al.* (CHARM Collaboration), Phys. Lett. **B180**, 303 (1986).

[156] P. Vilain *et al.* (CHARM-II Collaboration), Phys. Lett. **B335**, 246 (1994).

[157] G. P. Zeller *et al.* (NuTeV Collaboration), Phys. Rev. Lett. **88**, 091802 (2002), arXiv:hep-ex/0110059.